

Climate and land use controls over terrestrial water use efficiency in monsoon Asia

Hanqin Tian,^{1,2*} Chaoqun Lu,^{1,2} Guangsheng Chen,^{1,2} Xiaofeng Xu,^{1,2}
Mingliang Liu,^{1,2} Wei Ren,^{1,2} Bo Tao,^{1,2} Ge Sun,³ Shufen Pan^{1,2} and Jiyuan Liu⁴

¹ International Center for Climate and Global Change Research, Auburn University, Auburn, AL 36849, USA

² Ecosystem Dynamics and Global Ecology Laboratory, School of Forestry and Wildlife Sciences, Auburn University, Auburn, AL 36849, USA

³ Southern Global Change Program, USDA Forest Service, 920 Main Campus Drive, Raleigh, NC 27606, USA

⁴ Institute of Geographic Science and Natural Resources Research, Chinese Academy of Sciences, Beijing 100101, China

ABSTRACT

Much concern has been raised regarding how and to what extent climate change and intensive human activities have altered water use efficiency (WUE, amount of carbon uptake per unit of water use) in monsoon Asia. By using a process-based ecosystem model [dynamic land ecosystem model (DLEM)], we examined effects of climate change, land use/cover change, and land management practices (i.e. irrigation and nitrogen fertilization) on WUE in terrestrial ecosystems of monsoon Asia during 1948–2000. Our simulations indicated that due to climate variability/change, WUE in the entire area decreased by 3–6% during the study period, with the largest decrease of 6.8% in the 1990s. Grassland was the most sensitive biome to a drying climate, with a decrease of 16.2% in WUE in the 1990s. Land conversion from natural vegetation to croplands, accounting for 79% of the total converted land areas, led to a decrease in WUE, with the largest decrease of 42% while forest was converted to cropland. In contrast, WUE increased by more than 50% while cropland was converted to natural vegetation. Simulated results also showed that intensive land management practices could alleviate the decrease in WUE induced by climate change and land conversion. Changes in WUE showed substantial spatial variation, varying from the largest decrease of over 50% in northwestern China and some areas of Mongolia to the largest increase of over 30% in western, southern China, and large areas of India. To adapt to climate change and sustain terrestrial ecosystem production, more attention ought to be paid to enhance water use efficiency through land use and management practices, especially in the drying areas. Copyright © 2011 John Wiley & Sons, Ltd.

KEY WORDS climate change; land use/cover change; water use efficiency; Asia; dynamic land ecosystem model (DLEM)

Received 8 December 2010; Accepted 22 February 2011

INTRODUCTION

Monsoon Asia (MA) is a region largely influenced by the Asian monsoon climate and home of more than half the world's population (i.e. the people of South, Southeast, and East Asia). The distribution patterns of vegetation, soil, and water resources in MA have been shaped by both natural and anthropogenic disturbances for a long time period and thus are vulnerable to fast or sudden changes in climate and human activities [e.g. land use/cover change (LUCC) and management practices]. However, it is unclear how and to what extent climate change and intensive human activities have altered water use efficiency (WUE, amount of carbon uptake per unit of water use), a key measure for the functioning of terrestrial ecosystems in MA.

Since 1850, global surface air temperature has increased about 0.76 °C (Trenberth *et al.*, 2007) and is expected to increase by 1.5–6.4 °C by the end of the 21st century (Meehl *et al.*, 2007). Compared to other

regions of the world, surface air temperature in MA, modulated by Asian monsoon, has shown a large spatial range; a warming trend of 0.57 °C per 100 years was reported in India, while temperature decreased in some parts of the southeastern China (Lal *et al.*, 2001). The spatial and temporal patterns of temperature shift could have influenced regional precipitation regime. In the southern MA, precipitation decreased by 7.5% over the past century, while an increase of 6–8% was found in the northern and central MA (Trenberth *et al.*, 2007). This changing pattern of climate might have greatly altered the ecosystems functions (e.g. carbon, water, and nitrogen cycles) in this region (Tian *et al.*, 2003). Thus, large temporal and spatial variations in water use were expected to occur over the past decades. Till now, a great number of modelling and experimental studies have been conducted to investigate the interactions between carbon and water cycles in the context of climatic changes at different scales ranging from leaf, stand, site, region, to globe (Liang *et al.*, 1995; Law *et al.*, 2002; Davi *et al.*, 2006; Gerten *et al.*, 2008; Luo *et al.*, 2008; Wang *et al.*, 2008), but few of them considers the effects of human activity on WUE at a regional scale.

* Correspondence to: Hanqin Tian, International Center for Climate and Global Change Research; Ecosystem Dynamics and Global Ecology Laboratory, School of Forestry and Wildlife Sciences, Auburn University, Auburn, AL 36849, USA. E-mail: tianhan@auburn.edu

MA has experienced unprecedentedly rapid LUCC in the past century and this trend is likely to continue in the coming decades (Oikawa and Ito, 2001; Tian *et al.*, 2003). LUCC could greatly change the land surface biogeochemical and biophysical processes, leading to dramatic changes in water cycle and ecosystem productivity (Houghton and Hackler, 2003; Tian *et al.*, 2003, 2008, 2010a; Sakai *et al.*, 2004; Jarosz *et al.*, 2009). Associated with the change in land use and cover, land management practices such as irrigation, fertilizer and/or manure application, residue return, and tillage are recognized as important anthropogenic measures to improve crop yield, and hence, modify the carbon, water, and nitrogen cycles in agricultural land (Li *et al.*, 2006; Zhang *et al.*, 2006; Lu *et al.*, 2009), which covers around 20% of the total land area in MA. Although a few studies have assessed the impacts of environmental changes on carbon and water interactions (Luo *et al.*, 2008; Yu *et al.*, 2008; Wang *et al.*, 2008; Li *et al.*, 2010), none of them has addressed the changes in WUE in response to both natural and human perturbations at a regional scale. Thus, an integrated research is needed to understand how these environmental changes interactively affect carbon and water dynamics in MA.

Water has been identified as one of the most limiting factors for ecosystem functioning in MA due to limited and unevenly-distributed fresh water resources and high water demands for supporting its large cropland area, huge population, and rapid industrialization. For example, many of the rivers have dried up and been highly polluted in northern China due to water over withdrawal, over-use of fertilizer, and urbanization from the recent economic boom, resulting in large scale ecosystem degradations (Liu and Diamond, 2005). Terrestrial ecosystems in MA account for about 20% of the global net primary productivity (NPP) and for a similar proportion of carbon storage (Melillo *et al.*, 1993; McGuire *et al.*, 2001; Tian *et al.*, 2003). Plants and terrestrial ecosystems can respond to water stress in several ways: increasing water uptake from soils, increasing WUE, and reducing water losses (Hsiao, 1973; Waring and Running, 1998). To obtain a certain amount of NPP through less water use appeared as an important goal for maintaining ecosystem stability and sustainability in face of the changing environment in MA. As NPP and evapotranspiration (ET) are tightly coupled (Schimel *et al.*, 1997; Tian *et al.*, 2010a) and both are important functions for the terrestrial ecosystems, we adopted the definition of WUE as the ratio of ecosystem NPP to water loss through ET to reflect the close interactions between water and ecosystem productivity.

It is important to understand how human activities interact with climate change to affect WUE in MA. Such information is critical to policy makers in designing strategies for regional sustainability. In this study, a process-based ecosystem model [dynamic land ecosystem model (DLEM)] was used (1) to explore temporal and spatial patterns of WUE influenced by individual and combined changes in climate, LUCC, and

land management practices for the terrestrial ecosystems in MA during 1948–2000 and (2) to identify relative contributions of these factors to WUE variations in this region. According to the boundary defined in our study, MA is composed of 20 countries in South Asia (including Bangladesh, Bhutan, India, Nepal, Pakistan, and Sri Lanka); Southeast Asia (including Indonesia, Cambodia, Laos, Malaysia, Philippines, Thailand, Vietnam, Myanmar, and Afghanistan); and East Asia (including China, Japan, North Korea, South Korea, and Mongolia).

METHODS

Data description

To drive DLEM model, we collected and developed all the necessary model input data sets for MA during 1900–2000. The spatial resolution for these data sets was $0.5^\circ \times 0.5^\circ$. The spatially explicit data sets included time series of daily climate, annual LUCC, and land management practices. These data sets and other ancillary data such as potential vegetation map, cropping system information, soil property data, and topography maps are described as follows:

Historical climate. The half degree daily climate data (including average, maximum, minimum air temperature, precipitation, relative humidity, and shortwave radiation) during 1948–2000 were developed based on data set of NCEP/NCAR reanalysis 1 (<http://www.cdc.noaa.gov/cdc/data.ncep.reanalysis.html>). On the basis of the data from 1948 to 1970, we generated a set of randomly repeated detrended climate data to represent climate conditions during the period 1901–1947. Long-term average climate data from 1961 to 1990 were used to represent the initial climate state in 1900. Climate data from 1901 to 1947 have been used for model spin-up to eliminate system fluctuations caused by model shift from equilibrium mode to transient run, instead of being involved into analysis. During 1948–2000, precipitation decreased by 15.1 mm per decade (Figure 1). Before 1965, MA was wetter and warmer than most years in the late half of the 20th century. Precipitation amount significantly decreased in the whole study period, while no significant linear trend can be found in annual average temperature (Figure 1). Figure 2 displayed the changing trend of temperature and precipitation over the MA region. Annual average temperature during 1948–2000 increased in the north and northeast of MA, the southern India, and most areas of Southeast Asia, and decreased in the Tibetan Plateau and the northwest of MA (Figure 2(a)). In contrast, most areas of the northern and northeastern China, entire Mongolia, the southern India, and a few areas in Southeast Asia became drier. The wetter areas were centred in the south of East Asia, and most areas in Southeast Asia (Figure 2(b)). The drying area coincides with the warming area in the northeastern China, southern India, and Southeast Asia, which could deteriorate the shortage of water resources.

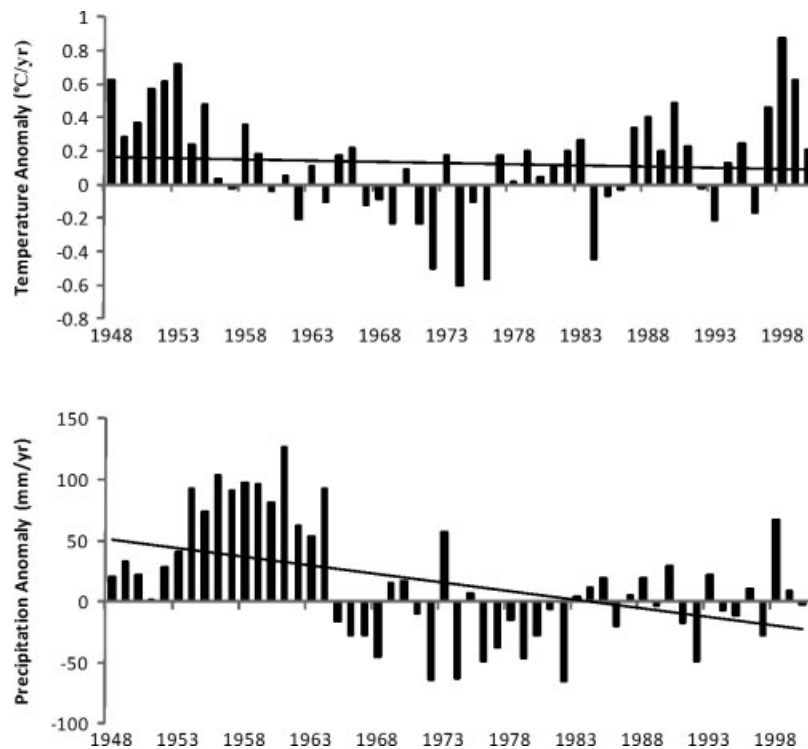


Figure 1. Anomaly of annual mean temperature and annual precipitation in monsoon Asia during 1948–2000 relative to 30-year average (from 1961 to 1990).

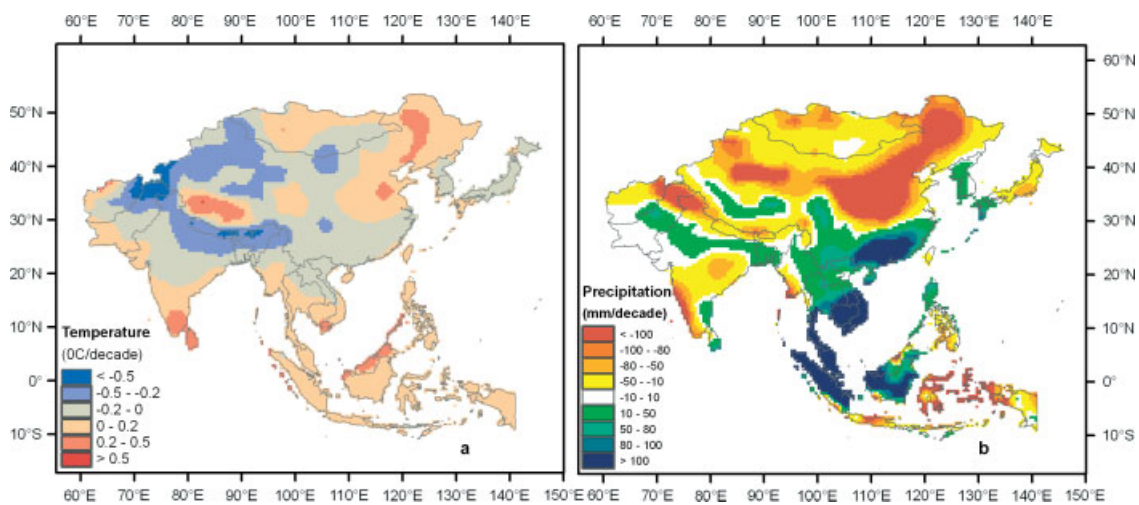


Figure 2. Changing trend of temperature ($^{\circ}\text{C}/\text{decade}$) and precipitation (mm/decade) across monsoon Asia during 1948–2000.

Historical LUCC. The major LUCC types in this study included land conversion from natural vegetation to cropland and natural vegetation recovery after cropland abandonment. Cropland maps in boolean format (1 for cropland, 0 for non-cropland) during 1900–2000 were developed by aggregating the 5-min resolution HYDE v3.0 global cropland distribution data (Goldewijk, 2001) into gridded data with a resolution of half degree. The data conversion followed a principle that total cropland area in the study region remained the same with the total area calculated from HYDE v3.0 percentage data (Liu and Tian, 2010). The LUCC data sets showed that during 1948–2000, 11% of land area in MA had experienced land conversions. Cropland abandonment accounted for

21% of total converted land area, while cropland establishment accounted for 79%. Till 2000, the increased cropland area was about 28.6% of the total cropland area in MA. Around 60.9% of newly established agricultural land was converted from forest, followed by shrubland and grassland, accounting for 23.0 and 16.6%, respectively (Figures 3 and 4). Most of land conversion (67%) occurred in a relatively drier period (1965–2000), the rest 33% of land conversion occurred during 1948–1964 when precipitation was higher than the long-term average (Figure 4).

Irrigation map. Contemporary irrigation map (Figure 4) in MA was developed according to global historical

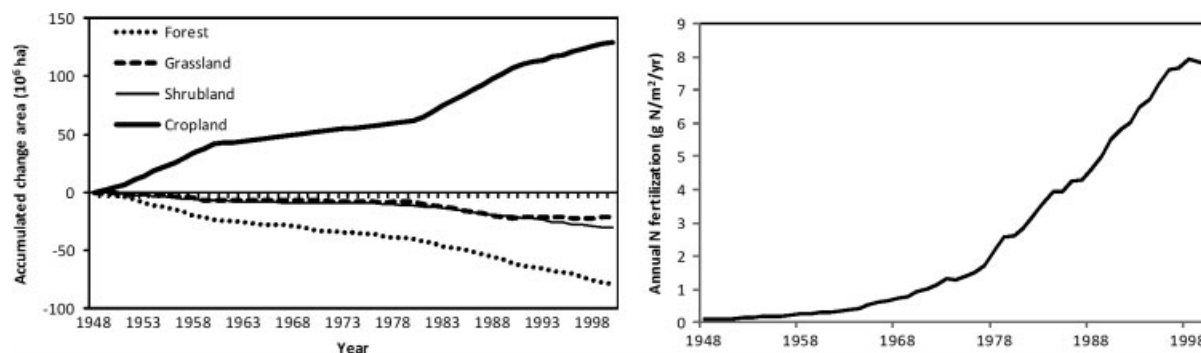


Figure 3. Accumulated change area of major biomes (left, 10^6 ha) and annual N fertilizer application rate in agricultural land (right, $\text{g N m}^{-2} \text{ year}^{-1}$) of monsoon Asia during 1948–2000.

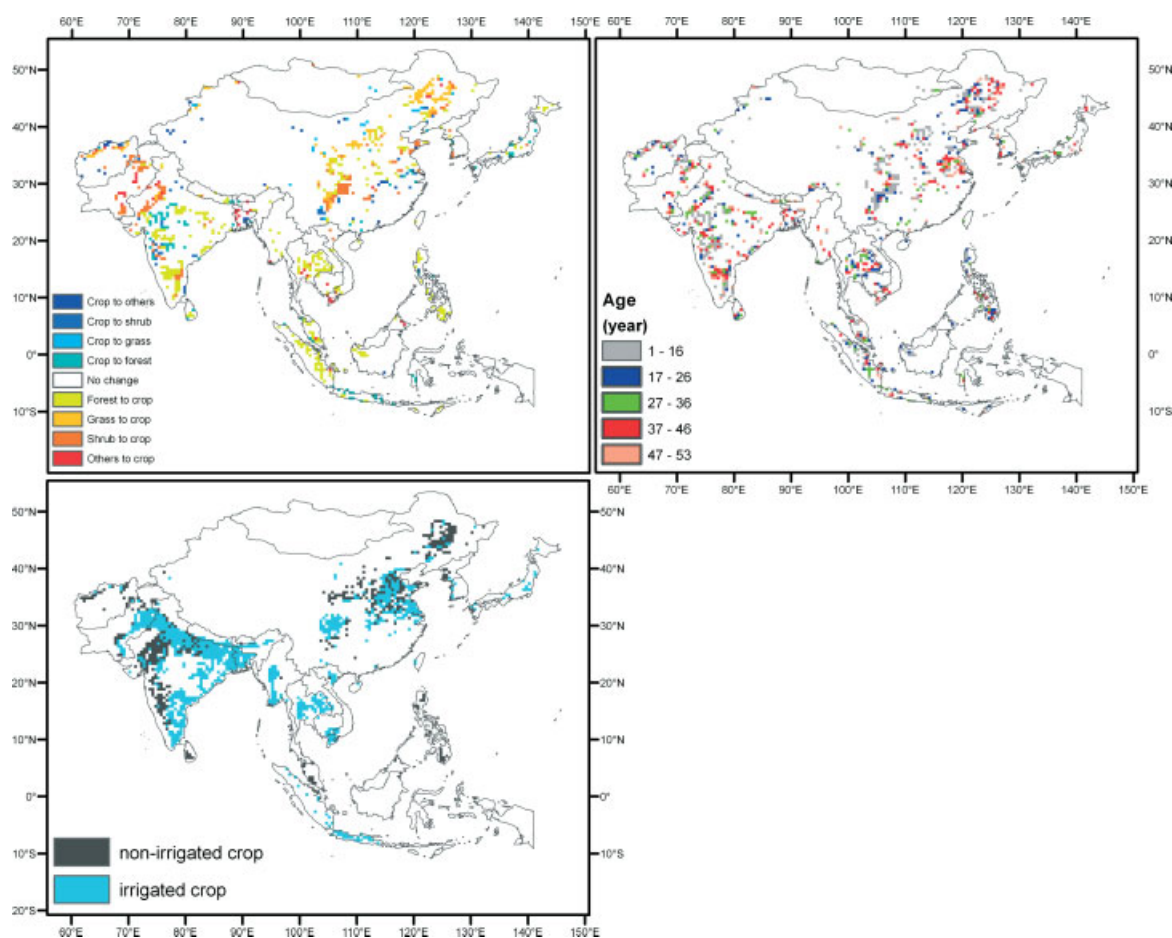


Figure 4. Land use/cover change in monsoon Asia during 1948–2000 (upper left), the age of each land conversion type by the year 2000 (upper right), and contemporary irrigation map in monsoon Asia (lower). *Others in upper left figure include desert, wetland, and tundra.

LUC database, global cropland distribution map, and global irrigated percentage map (Goldewijk, 2001; Leff *et al.*, 2004; Siebert *et al.*, 2007). Crop-specific irrigated area (rice paddy field and irrigated dry farmland) was identified according to the above information. Then, the contemporary irrigation map was produced by combining global irrigation map, crop-specific irrigated area, and global cropland records in 1999 (0.25–0.28 billion ha, or 16–18% of cropland area). During the study period, irrigated area increased by 33.5×10^6 ha, but its proportion to total cropland area decreased from 57% to 48%. However, in this study, the changes in total irrigated area

were caused by changes in cropland distribution, rather than by shifts between irrigated and non-irrigated zones.

Nitrogen fertilization data set. Historical nitrogen fertilization rates in China were estimated based on census data at county level and tabular data at provincial level (Ren *et al.*, 2011). Consumptions of nitrogen fertilizers from 1961 to 2005 for other countries in MA were derived from the FAO statistic database (<http://faostat.fao.org>). We then calculated annual fertilization rate (g N m^{-2}) as the ratio of national fertilizer application amount to total cropland area in this

country. Average fertilization rate in cropland increased from nearly 0 in 1948 to 8.6 g N m⁻² year⁻¹ in 2000 for the entire MA, but varied greatly across the region (Figure 3).

Cropping system and crop phenology. Nine major crop types (i.e. wheat, corn, soybean, cotton, groundnuts, millet, barley, sorghum, and rice) and three rotation types (one, double, and triple harvesting) in MA were simulated in this study. On the basis of the global distribution map of major crops at a spatial resolution of 5 arc min (~10 km) (Leff *et al.* 2004), we generated major crops' distributions at a half degree resolution. The MODIS 8-day LAI products (MOD15) during 2000–2008 (<http://modis.gsfc.nasa.gov/data/dataproduct>) in conjunction with observation and survey data sets (e.g. China's agriculture meteorological stations), were used to identify rotation type and the contemporary patterns of phenologic metrics. We have applied such a method into historical studies over the globe including Southern United States (Tian *et al.*, 2010a), North American continent (Tian *et al.*, 2010b; Xu *et al.*, 2010), and China (Ren *et al.*, 2011; Tian *et al.*, 2011a, 2011b).

Potential vegetation. Potential vegetation map was generated based on multiple data sources. We first combined the MODIS global land cover map (<http://modis-land.gsfc.nasa.gov/landcover.htm>) with the global potential vegetation map developed by Ramankutty and Foley (1999) to derive the first draft of the potential vegetation map. Both data sets (with 1 km × 1 km resolution) were aggregated using the majority rule and their vegetation types were regrouped to match the corresponding plant functional types defined in DLEM. Next, the global C₄ grassland percentage map developed by Still *et al.* (2003) was used to determine the distribution of C₄ grassland in the study region. Finally, we identified the wetland area based on the half degree-resolution Global Lakes and Wetlands Database developed by Lehner and Döll (2004).

Soil properties. We obtained the spatial maps for soil bulk density, soil pH, and texture (i.e. percentage of clay, sand, and silt particles) in the study region from the International Satellite Land Surface Climatology Project Initiative II Data Collection (distributed by the Oak Ridge National Laboratory Distributed Active Archive Center, <http://daac.ornl.gov/>), which provided spatially-explicit global soil information. These soil data were coordinated by the data and information system of the International Geosphere–Biosphere Programme.

Topography. Topography maps required by DLEM include the elevation, slope and aspect of the study region. We first aggregated the Global 30 Arc Second Elevation Data (GTOPO30), which were developed by the United States Geological Survey (Bliss and Olsen, 1996), to half degree resolution to develop the digital elevation model (DEM) for the study region. Then

the half degree-resolution aspect and slope maps were derived from the DEM data.

Model description

Overview of DLEM. The DLEM is a highly integrated, process-based terrestrial ecosystem model that aims at simulating the structural and functional dynamics of land ecosystems affected by multiple factors including climate, atmospheric compositions (CO₂ and O₃), precipitation chemistry (nitrogen composition), natural disturbance (fire, insect/disease, hurricane, etc.), LUCC, and land management practices (harvest, rotation, fertilization, irrigation, etc.). DLEM includes five core components (Figure 5) such as (1) biophysics, (2) plant physiology, (3) soil biogeochemistry, (4) dynamic vegetation, and (5) land use and management (Tian *et al.* 2010a). This model has been extensively calibrated against various field data covering forest, grassland, and cropland from the Chinese Ecological Research Network, US LTER (Long Term Ecological Research) sites, and AmeriFlux network. DLEM has been used to simulate the effects of climate variability and change, atmospheric CO₂, tropospheric O₃, nitrogen deposition changes, and LUCC on the pools and fluxes of carbon and water in China (Chen *et al.*, 2006; Ren *et al.*, 2007, 2011; Liu *et al.*, 2008; Tian *et al.*, 2011a, 2011b), United States (Tian *et al.*, 2008; 2010a; Zhang *et al.*, 2008a), and North America (Tian *et al.*, 2010b; Xu *et al.*, 2010).

The algorithms used to estimate gross primary productivity (GPP) are built upon a modified Farquhar's model (Farquhar *et al.*, 1980; Collatz *et al.*, 1991; Sellers *et al.*, 1992; Bonan, 1996; Oleson *et al.*, 2004). Leaf photosynthesis is closely linked to stomatal conductance, and hence composes an integral part of surface energy flux. DLEM scales leaf-level carbon assimilation rate up to the whole canopy combined with projected leaf area indices and absorbed photosynthetic active radiation specific to sunlit and shaded leaves, respectively. Specifically, canopy GPP, stomatal conductance (g_n), NPP, and autotrophic respiration (R_a) are estimated as

$$\begin{aligned} \text{GPP} &= f(T, g_n, \text{CO}_2, \text{ppf}, K, N) \\ g_n &= \max(g_{\max}, f(\text{ppdf})f(T)f(\text{VPD})f(W)f(\text{CO}_2), \\ &\quad g_{\min}) \\ \text{NPP} &= \text{GPP} - R_a \\ R_a &= \Sigma f(\text{GPP}, T, C_i, N_i) \end{aligned} \quad (1)$$

where, GPP is a function of air temperature (T), enzyme (including Rubisco, light, and carbohydrate export-limited enzymes) kinetics (K), photosynthetic photo flux (ppf), stomata conductance (g_n), canopy surface CO₂ concentration (CO₂), and leaf nitrogen level (N); g_{\min} and g_{\max} are the plant functional type-specific minimum and maximum canopy conductance, respectively; $f(\text{ppdf})$ is the impact function of ppf density (radiation); $f(\text{VPD})$ is the impact function of vapour pressure deficit at the canopy surface; $f(W)$ is the impact function of soil

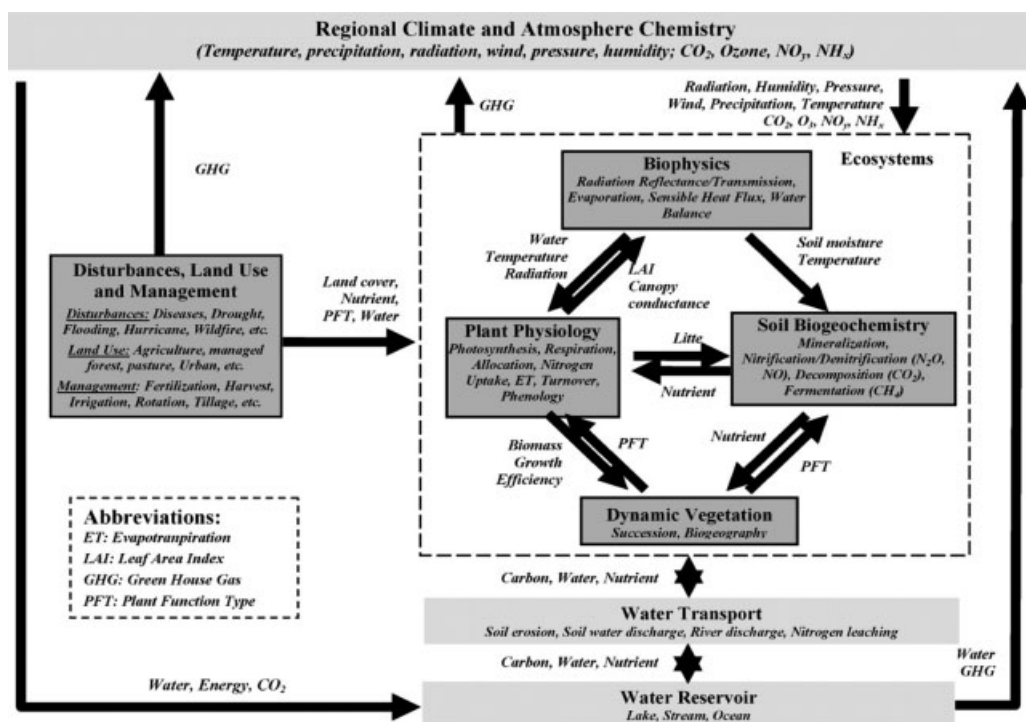


Figure 5. Structure and key components of Dynamic Land Ecosystem Model (DLEM).

moisture; $f(\text{CO}_2)$ is the impact function of atmospheric CO_2 concentration; NPP is calculated as the difference between GPP and R_a ; R_a is a function of air temperature, GPP, carbon content in component i (i , 1: leaf; 2: stem for herbaceous species, heartwood and sapwood for woody species; 3: fine root; 4: coarse root; 5: reproduction), and nitrogen content in component i (N_i).

Evapotranspiration in DLEM primarily includes four major components: (1) plant transpiration, (2) canopy evaporation, (3) soil evaporation, and (4) canopy and land surface snow sublimation. DLEM algorithms for specifically simulating these components of ET have been described in detail by Tian *et al.* (2010a). Temperature and precipitation amount are critical factors in the estimation of ET by affecting surface wetness, soil moisture, as well as stomatal conductance.

Impacts of land use change. DLEM assumes that all the biomass will be removed when natural vegetation is converted to cropland. A part of vegetation carbon may enter product pools with lifetimes of 1, 10, and 100 years and the proportion of these carbon transfer is determined by vegetation type (Houghton *et al.*, 1983; McGuire *et al.*, 2001; Tian *et al.*, 2003), while the other part may be burned or left on the ground or in the soil. The carbon left in the soil will gradually decompose along with mineralization of organic nitrogen. Accompanying carbon redistribution after land use change, the ecosystem nitrogen and water cycles will be correspondingly changed, which will in turn feedback to ecosystem recovery and development. This coupling approach differs from book-keeping or statistical estimation methods that are commonly used to assess land use change effects. An agricultural module is specifically developed in DLEM

to retrieve the trajectory of cropland establishment and to simulate the impacts of environmental factors and management activities (such as seeding, planting, irrigation, fertilization, tillage, rotation, genetic improvement, and harvest) on agricultural ecosystem functioning (Ren *et al.*, 2011). On contrary, when cropland is abandoned, natural vegetation will grow back and the simulated recovery is controlled by environmental factors. DLEM uses a process-based modelling scheme to fully track the successional stages of natural vegetation recovery and the associated carbon and water dynamics after land use change.

Land management practices. In this study, nitrogen fertilizer application, irrigation, harvest, and rotation were considered as the major management practices applied in croplands of MA. However, we only investigate the impacts of nitrogen fertilization and irrigation on NPP and ET as rest of the management practices cannot be tracked due to lack of long-term records and are assumed to be constant during the study period. In DLEM, prescribed nitrogen fertilizer uses will directly modify soil nutrient availability, and therefore, alter NPP, ET, and WUE in the managed ecosystems. Irrigated area is prescribed by contemporary irrigation map. Irrigation is assumed to occur when the moisture of top soil in irrigated cropland drops below 30% of the maximum available water (i.e. field capacity minus wilting point) during the growing season and irrigated water is assumed to be sufficient enough to reach soil field capacity.

Model parameterization and validation

Before simulation, we selected a wide range of long-term observational sites which covered all the natural

plant functional types and crop types identified in MA to calibrate the model. The DLEM's performance to simulate impacts of climate, LUCC, and land management on carbon storage, ET, NPP, and greenhouse gas emissions has been extensively evaluated against field observations and regional inventory data in China (Liu *et al.* 2008; Ren *et al.* 2011; Tian *et al.* 2011a, 2011b), the Southern United States (Tian *et al.* 2010a), and North America (Schwalm *et al.* 2010; Tian *et al.* 2010b; Xu *et al.* 2010). It turned out that DLEM performed well in simulating the magnitude and temporal variation of carbon and water fluxes in a wide variety of land ecosystem types at both site and regional scales. DLEM's capability in capturing the impacts of drought has also been proved in the North American Carbon Program (NACP) site synthesis project (Schwalm *et al.* 2010).

In this study, we further evaluated DLEM's performance in simulating NPP across MA by comparing DLEM-simulated results with MODIS NPP products (Zhao *et al.*, 2005) and field observational data [Global Primary Production Data Initiative (GPPDI) Olson *et al.*, 2001]. The spatial pattern of the modelled NPP is consistent with that of MODIS NPP. However, the algorithms of MODIS for estimating NPP are not well calibrated for cropland. A comparison of NPP measured at eddy covariance flux towers in China's cropland with MODIS-estimated NPP (Zhang *et al.*, 2008b), indicated that MODIS has significantly underestimated the cropland NPP, which partly explained the higher estimates from the DLEM relative to MODIS products. For bare land such as Taklamakan Desert in West China, there is no NPP data calculated from MODIS and we excluded those areas from analysis. Here, we adopted two statistical indices to measure the deviation of estimates from the DLEM model and other approaches, such as satellite-derived or field-observed fluxes. The first one is square root of the mean square error of predictions (RMSEP) (Equation (2)), which indicates the absolute fit of the model to the data points (Haefner, 2005). The lower RMSEP is, the better model predicts.

$$\text{RMSEP} = \sqrt{\frac{1}{n} \sum (x_i - y_i)^2} \quad (2)$$

where x_i , y_i are the model outputs and observations (or estimates from satellite products in this study) at the i th time point or in the i th grid, respectively and n is the number of paired data points. The second index we used is inequality coefficient, U , developed by Theil (1961). It standardized RMSEP to a range of 0–1 by dividing the sum of mean square prediction and mean square observation (Equation (3)). Smaller U indicates accurate model estimates.

$$U = \frac{\sqrt{\frac{1}{n} \sum (x_i - y_i)^2}}{\sqrt{\frac{1}{n} \sum x_i^2} + \sqrt{\frac{1}{n} \sum y_i^2}} \quad (3)$$

The fitted line between DLEM-simulated and MODIS-derived NPP was close to the 1:1 line with a high slope

of 1.01 and a low U coefficient of 0.22. (Figure 6(a)–(c)). GPPDI data products include above-ground, below-ground, and total NPP for more than 1000 measurements in Asia, which were compiled by Olson *et al.* (2001). Most of the GPPDI data came from four major vegetation types: boreal forest, temperate forest, tropical forest, and grassland. We extracted the DLEM-estimated NPP from our regional simulation outputs to match the geographic information of these sites. We found a good agreement between the simulated and measured NPP for different plant functional types (Figure 6(d)). The fitted lines between simulated and measured NPP have slopes between 0.82 and 1.05, and U value ranging from 0.20 to 0.30.

Besides, in our previous research (Liu *et al.*, 2008; Tian *et al.*, 2010a), the DLEM-simulated ET was evaluated against observations in China and United States. However, few sites in tropical area have been used for model test. Therefore, in this study, we selected one of AsiaFlux sites located in Palangkaraya drained forest (PDF) of Indonesia and compared DLEM-estimated ET with observed ET using eddy covariance technique from 1 January 2002 to 31 December 2005. It showed that DLEM was capable of well capturing both the magnitude and seasonal/daily patterns of ET (Figure 7(a) and (b)). The annual average ET during this period was simulated as $1290 \pm 26 \text{ mm year}^{-1}$, falling in the range of observational data, $1314 \pm 30 \text{ mm year}^{-1}$. The regression line is very close to 1:1 line with a slope of 1.03, an RMSEP of 0.74 mm day^{-1} and a U of 0.10. Almost all the simulated ET fell in the $\pm 50\%$ range of observed values. However, DLEM appeared to overestimate daily ET of tropical forest in the dry season (from June to August, marked with an oval in Figure 7(a)). This is probably caused by the model assumption of multiple soil layers which may over-buffer the changes of soil water content, leading to a less sensitive model estimate when drought occurred. Apart from the daily pattern, annual ET observation from a couple of eddy covariance flux sites and meteorological stations were also compiled to verify model's performance (Figure 7(c)). It indicated that DLEM estimates are statistically acceptable compared to observed values with a high slope of 1.02, RMSEP of $138.6 \text{ mm year}^{-1}$ with annual ET ranging from 500 to 1500 mm, and a U of 0.07.

Simulation experiment design

In this study, we conducted 12 simulation experiments (Table I) to examine the responses of carbon, water fluxes, and WUE to climate change, LUCC, and land management practices (irrigation and fertilization) in the terrestrial ecosystems of MA over the last half of the 20th century. Experiment I (CLM), II (Prec), and III (Temp) allowed all climate factors, precipitation alone, and temperature alone to change from 1901 to 2000, respectively, while land use pattern remained at the level of 1900; In Experiment IV (LUCC) and V(LUCC-Nfer), land conversion alone and both land conversion and nitrogen fertilizer application were subject to changes along 1901 to

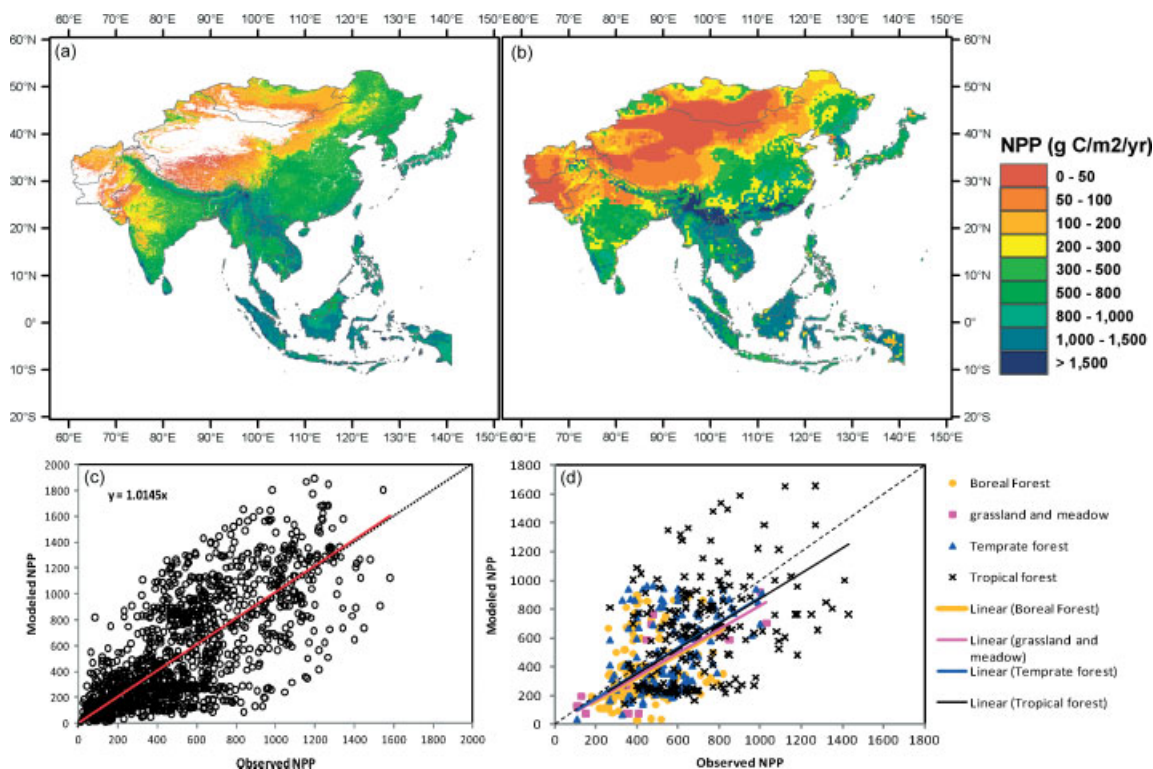


Figure 6. Spatial patterns of MODIS-derived NPP (a) and simulated NPP (b) in monsoon Asia during 2000–2006 and comparisons of the simulated NPP with MODIS–NPP (c) and field observational data during 1980–2000 (d) (unit is $\text{g-C m}^{-2} \text{ year}^{-1}$). The solid line is linear trend with regression equation and the dash line is 1 : 1 line. The data points in (c) are randomly sampled from MODIS-derived NPP and modelled estimates in the same period. Model performance is statistically accepted ($y = 1.0145x$, $U = 0.22$). In comparison with observed NPP data, the indices used for measuring model validity in each biome type in Figure d are: boreal forests ($y = 0.823x$, $U = 0.30$, $N = 153$), grassland and meadow ($y = 1.053x$, $U = 0.20$, $N = 14$), temperate forests ($y = 0.922x$, $U = 0.20$, $N = 119$), and tropical forests ($y = 0.913x$, $U = 0.23$, $N = 195$).

2000, respectively, with climate condition constant at the level of 1900; Experiment VI (CLM-LUCC-Nfer) combined the changes in all the above factors throughout the last century. All these experiments set up irrigated cropland according to the unchanged contemporary irrigation map, but the real irrigated area varied because of changes in cropland distribution (Figure 4). We run DLEM from 1900 to 2000 and analysed the impacts of climate, land use, and management practices during 1948–2000 as the reliable daily climate data began from the year of 1948. To eliminate the inherent ecosystem fluctuation and legacy effects from the time period before 1948, we implemented six more simulation experiments (VII–XII) corresponding to the ‘manipulated’ experiments I to VI, to distinguish the nonlinear system behaviour. In those experiments, the changing forces varied during 1901–1948, and thereafter kept constant at the level of 1948. The difference between each pair of simulation experiments with and without changes after 1948 can reflect the individual or combined model-estimated effects of the altering climate, land use, and land management practices on the variables of interest.

To select an initial point is critical for the simulated results but there is no well-accepted idea on what time is appropriate for initializing the model run (McGuire *et al.*, 2001; Mu *et al.*, 2008). In this study, before transient run, we used climate data, atmospheric CO₂ concentration, O₃ AOT40 index, nitrogen deposition, land use types,

and land management practices in 1900 to run the model until equilibrium state. Then, we spun the model to reach a dynamic equilibrium. For experiments without transient climate, a 300-year spin was carried out with the climate data in 1900. Climate data during 1901–1947 was repeatedly selected for a 235-year spin for climate-transient experiments. After spin-up, the input data sets were fed into the model in transient mode.

To address the magnitude of NPP, ET, and WUE change driven by the individual or combined factors, we calculated the percent change as the ratio of absolute change values (difference between each pair of simulation experiments) to ‘background’ variable values, which were driven by inherent system behaviour rather than by environmental changes, i.e. output from corresponding experiment VII–XII during the same time period (Table II). In addition, we calculated the changes in NPP, ET, and WUE estimated by experiment IV (LUCC), V (LUCC-Nfer) and their corresponding ‘background’ experiments (X and XI) to examine the impacts of nitrogen fertilizer application. From these four experiments, the carbon and water fluxes in irrigated and non-irrigated cropland have been distinguished to investigate how irrigation and fertilization combined to affect NPP, ET, and WUE.

Statistical analysis

Regression analysis was used in this study to evaluate DLEM model performance at site and regional

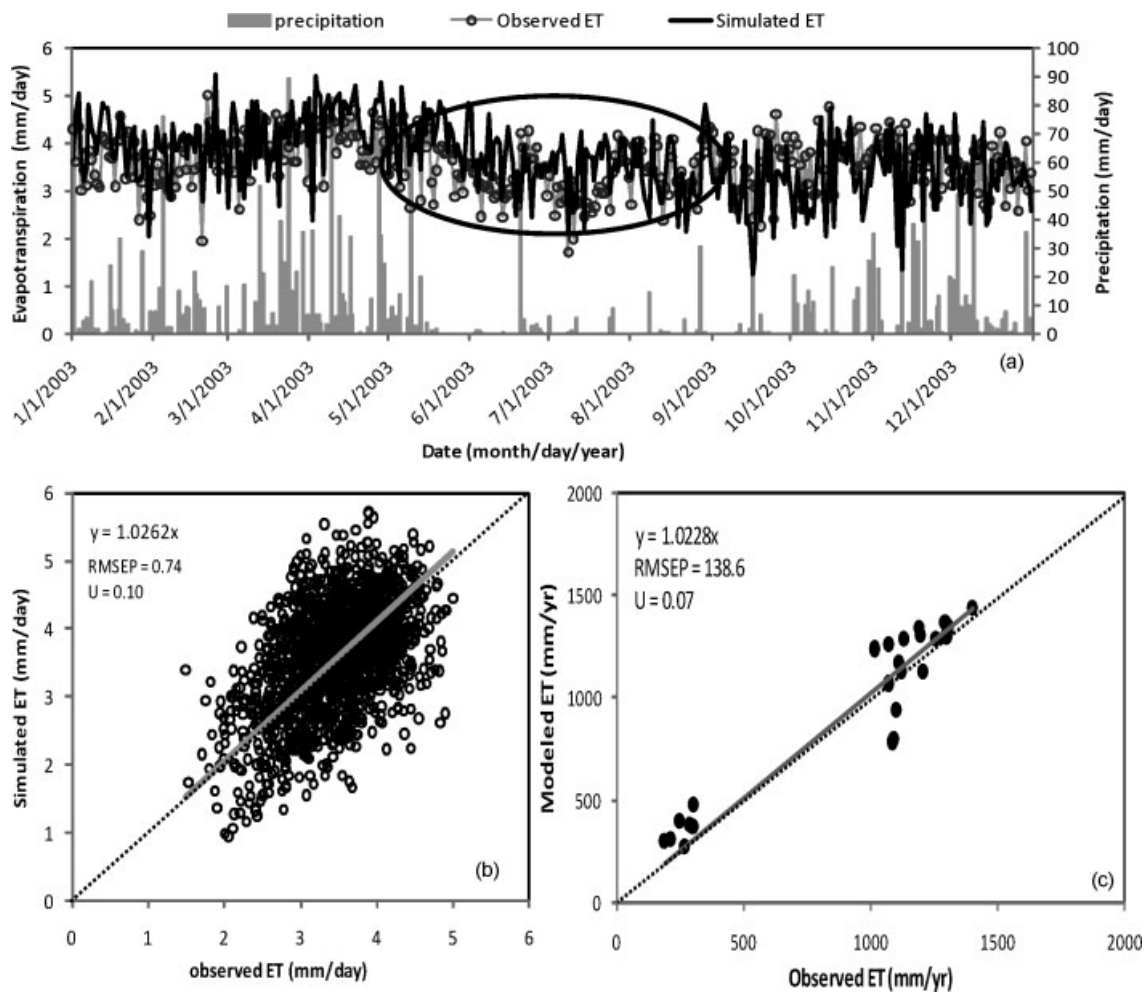


Figure 7. Comparison of DLEM-simulated and field-observed ET at flux tower of Palangkaraya drained forest (PDF) in Indonesia: (a), daily pattern of precipitation, simulated, and observed ET (unit: $\text{mm}\cdot\text{day}^{-1}$) during 1 January–31 December 2004; (b), scatter plot of simulated and observed ET during 1 January 2002–31 December 2005. (c) is the simulated ET compared with observations in monsoon Asia, including boreal mixed forest in Changbai Mountain, China (Zhang *et al.*, 2009), conifer-hardwood mixed forest in Teshio CC-LaG experiment site, Japan (AsiaFlux, http://asiaflux.yonsei.ac.kr/network/009TSE_1.html), rainforest in Lambir Hills National Park, Malaysia (Lim *et al.*, 2009), tropical peat swamp forest in PDF, Indonesia (AsiaFlux, http://asiaflux.yonsei.ac.kr/network/008PDF_1.html), cropland in Tongyu, China (CEOP, http://www.eol.ucar.edu/projects/ceop/dm/insitu/sites/ceop_ap/Tongyu/Cropland) and 12 meteorological stations in China (Song *et al.*, 2010). The grey solid lines in (b) and (c) are linear trend with regression equation and the dash line is 1:1 line.

levels. Correlation analysis was applied to identify the relationships between environmental factors and model output variables. All the statistical analyses were conducted by using SPSS 17.0 for Windows XP.

RESULTS

Impacts of climate change on WUE

Our model simulation indicated that due to climate change, WUE decreased by $0.023 \text{ g C kg}^{-1} \text{ H}_2\text{O}$ during 1948–2000, equivalent to 3.64% of annual average WUE in MA. WUE varied over time, however, with the largest decrease of 6.81% in the 1990s (Table II). Both NPP and ET decreased during this time period, but the reduction in NPP was faster than that in ET, which led to a decrease in WUE. NPP declined by $18.93 \text{ g C m}^{-2} \text{ year}^{-1}$ (or $0.39 \text{ Pg C year}^{-1}$) over the past half century, accounting for 3.9% of annual average NPP. ET reduced by 23.96 mm, or 3.53% of the average values for the entire study

period. Likewise, the largest decreases in NPP and ET were found in the 1990s, with decrease rates of 6% and 6.8%, respectively (Table II). However, substantial variation existed in climate impacts on WUE across the region and the relatively small change over entire MA might be related to the sum of changes with different directions. The areas with great changes are paid more attention in this study.

Among all the biome types in MA, grassland showed the highest response of WUE to climate changes, with average decrease rates of 8–10% during 1948–2000 and 16.23% in the 1990s, respectively. Cropland was the second, with WUE decrease by 2.97% during 1948–2000 and 8.47% in the 1990s. WUE in forest and shrubland was less sensitive to climate, with a slight decrease of 0.82% and an increase of 0.79%, respectively.

For the entire MA, NPP, ET, and WUE were decreased from 1948 to 2000, with the highest decreases occurring in recent decades (Figure 8), which was consistent with the decreasing trend of precipitation. We found that NPP

Table I. Design of simulation experiments in this study.

Experiments	Precipitation	Temperature	Land use	Irrigation	Fertilization
I CLM	1900–2000	1900–2000	1900	Yes	No
II Prec	1900–2000	1900	1900	Yes	No
III Temp	1900	1900–2000	1900	Yes	No
IV LUCC	1900	1900	1900–2000	Yes	No
V LUCC-Nfer	1900	1900	1900–2000	Yes	1900–2000
VI CLM-LUCC-Nfer	1900–2000	1900–2000	1900–2000	Yes	1900–2000
VII CLM-bgd	1900–1948	1900	1900	Yes	No
VIII Prec-bgd	1900–1948	1900	1900	Yes	No
IX Temp-bgd	1900	1900–1948	1900	Yes	No
X LUCC-bgd	1900	1900	1900–1948	Yes	No
XI LUCC-Nfer-bgd	1900	1900	1900–1948	Yes	1900–1948
XII CLM-LUCC-Nfer-bgd	1900–1948	1900–1948	1900–1948	Yes	1900–1948

Notes: CLM, LUCC and Nfer are abbreviations for climate, land use/cover change and nitrogen fertilizer application, respectively. bgd is abbreviation for background simulation experiment, where changing factors were assigned to be constant after the year 1948 to reflect the nonlinear system behaviour and legacy effects derived from environmental changes before 1948.

Table II. Decadal changes in NPP, ET, and WUE in the entire monsoon Asia caused by climate, LUCC, and nitrogen fertilizer application relative to control simulation experiment.

		NPP (%)	ET (%)	WUE (%)
CLM	1950s	-0.04	0.71	0.32
	1990s	-6.82	-6.00	-6.81
LUCC	1950s	-0.54	0.64	-1.00
	1990s	-3.32	1.40	-3.30
LUCC + Nfer	1950s	-0.43	0.34	-0.47
	1990s	3.23	2.20	2.28
CLM + LUCC + Nfer	1950s	-0.44	1.08	-0.13
	1990s	-3.56	-3.46	-4.63

was stimulated by increased precipitation amount and relatively higher temperature during 1954–1964, even though the effects of changes in other climatic variables counteracted the rise of NPP in this period (Figure 9(a)). However, ET increase resulted from large amount of precipitation was partly offset by the temperature effects during this time period (Figure 9(b)), while both precipitation and temperature contributed to the increases in WUE, i.e. ecosystems showed more efficient in using water to obtain carbon in this time period. After 1964, climate change resulted in decreases in NPP, ET, and consequent WUE. This implied that climate change played a critical role in decreasing WUE of terrestrial ecosystems in MA, especially in recent decades, which was primarily caused by less rainfall and warmer environment emerged in this region.

Increased NPP and ET were found in central Pakistan, western and southern China, and Vietnam because the warming and/or wetting environment in these areas might favour plant growth (Figure 10). In contrast, drying environments in the northern, northwestern China and large areas of Mongolia led to reductions in NPP and ET. Increased WUE in the western and southern China was mainly due to wetting-stimulated NPP, while increased WUE in most areas of India might be related to lower ET in drying and cooling climate conditions. Decreases

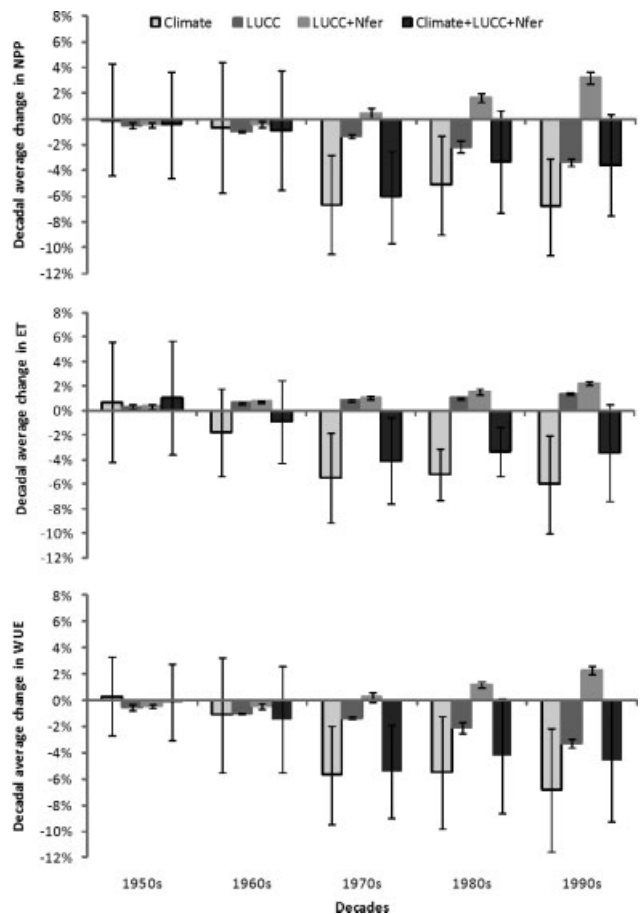


Figure 8. Decadal changes in NPP, ET, and WUE due to climate change, LUCC, and land management practices in monsoon Asia during 1948–2000. Error bar is standard deviation of annual change in each decade.

in WUE in Northwest China and some areas of Mongolia during 1948–2000 were probably caused by the fact that drought-induced reduction in NPP overwhelmed the decline of ET across this area (Figure 10(c)). The northern MA including North China and entire Mongolia appeared more sensitive to climate change than other regions did, while the southern MA including part of

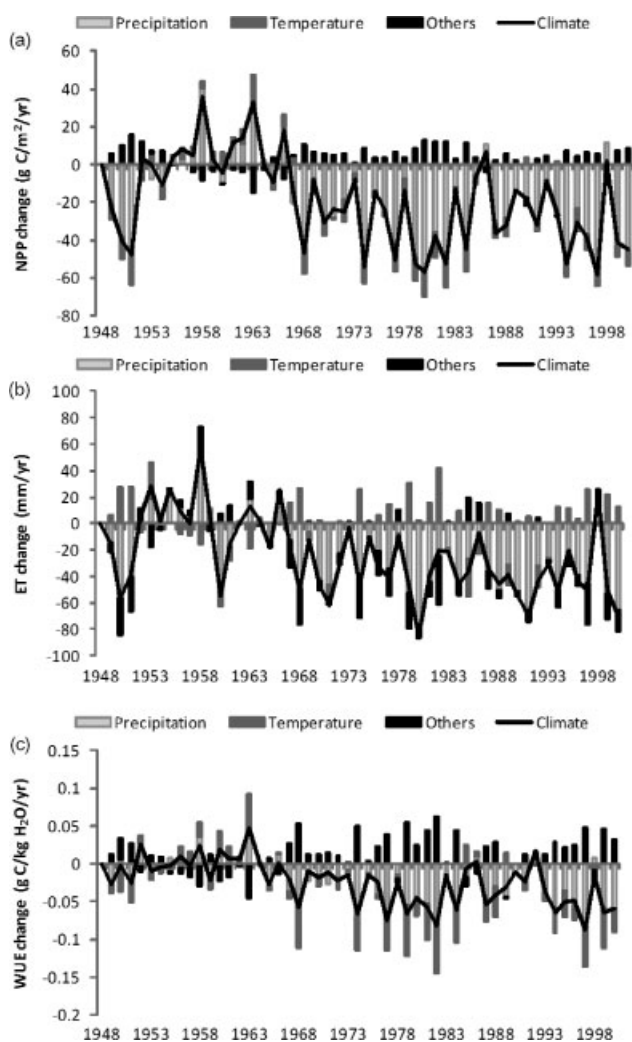


Figure 9. Impacts of climate change (temperature, precipitation, short-wave radiation, and relative humidity) on annual NPP (a), ET (b), and WUE (c) in monsoon Asia over the period 1948–2000.

South China and Southeast Asia was less sensitive to climate change. One probable reason of this insensitive response of the southern MA was that increased rainfall and warming climate might not be able to significantly stimulate plant growth, ET, and thus WUE in this region where water availability and air temperature were not major limiting factors.

Impacts of LUCC and land management practices on WUE

Responses of carbon and water fluxes to land conversion were enlarged along time because cropland kept expanding and area covered by natural vegetation, such as forest, shrubland, and grassland, continued to shrink in MA over the study period (Figure 3). We found that land conversion alone significantly decreased ecosystem productivity and the consequent WUE as the cropland establishment dominated among all kinds of conversion types in MA over the past century. However, the practices of land management have turned this reduction into increase in the latest decades (Figure 8).

Our simulations indicated that combined with nitrogen fertilizer uses and irrigation, land conversion from natural vegetation to cropland, accounting for 79% of converted land area, generally decreased WUE. The largest decreases occurred for the conversion from forest to cropland, with a decrease of 42%, followed by shrubland to cropland, and grassland to cropland, with WUE decreasing by 29 and 19%, respectively. However, the conversion from cropland to natural vegetation types, covering the rest 21% of land conversion, largely augmented WUE, with changing rate found to be more than 50% in all conversion types (Table III).

It is notable that the above change rates are calculated in the area where land use change occurred, covering 11% of entire MA, since the year when land conversion took place in each grid cell. Therefore, extrapolating the changes in carbon and water fluxes to the entire region and the whole study period, our simulations showed that the impacts of land conversion and management practices were small compared to continent-wide climate effects. Our results implied that decrease in WUE averaged to -1.56% due to land conversion alone, while incorporation of nitrogen fertilizer uses overturned the reduction and resulted in a slight increase of 0.53% , with largest increase of 2.28% in the 1990s (Table II). However, climate variability and changes remained to be a predominant factor determining the WUE change of terrestrial ecosystems for the entire MA region. Although LUCC played a critical role in some areas, it is not large enough to shape the WUE pattern on continental scale. Caused by land conversion and land management practices, the increase in NPP concentrated in Southeast China, South, and Southwest India (Figure 11(a)), and it was mainly related to the land conversion from low-productivity vegetation to high-productivity types, such as cropland to forest, shrubland to managed cropland, and others (e.g. desert and tundra) to managed cropland. In contrast, large areas of cropland establishment in the northern part of South Asia, including Pakistan, Afghanistan, and India, and intensive deforestation in Southeast Asia led to significant decrease in NPP. Meanwhile, ET kept rising in most land conversion area because the large portion of cropland establishment was usually followed by irrigation practices (Figure 11(b)). WUE increased in most converted areas of China and scattered areas of India because NPP increase in these regions surpassed rise of ET, while large areas of North India, Pakistan, Afghanistan, and Southeast Asia experienced decline in WUE because NPP in the newly established cropland within these regions was much lower compared to its original vegetation cover, and most of them were not subjected to irrigated water supply (Figure 4) and tended to demand more water to sustain plant growth (Figure 11(c)).

Our study proved that effects of land conversion on carbon/water fluxes and WUE were modified by land management practices (Figure 12). Nitrogen fertilizer application largely enhanced NPP, while irrigation practice significantly raised ET level. Overall, WUE was

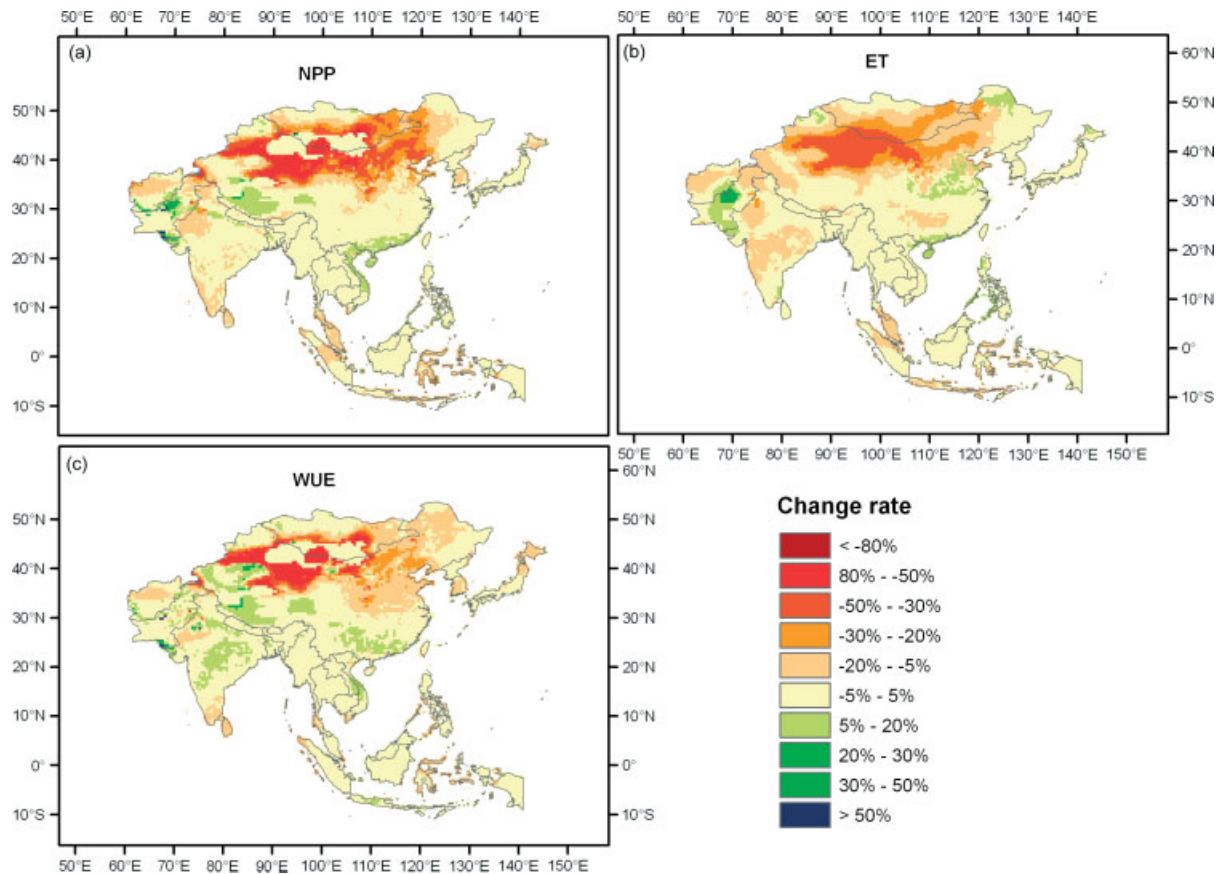


Figure 10. Changes in mean annual NPP (a), ET (b), and WUE (c) due to climate change across monsoon Asia during 1948–2000.

Table III. percent changes in annual NPP, ET, and WUE induced by LUCC and management practices for each land conversion type occurred in monsoon Asia during 1948–2000.

Land conversion type	Area (%) ^b	Change percentage ^a		
		NPP (%)	ET (%)	WUE (%)
Crop to others	3.23	53.98	-20.47	72.31
Crop to shrub	5.40	5.86	-42.54	74.26
Crop to grass	2.48	58.00	6.23	50.96
Crop to forest	9.61	34.78	-25.74	56.56
Forest to crop	43.82	-34.20	30.71	-41.55
Grass to crop	12.12	-25.15	-11.56	-18.90
Shrub to crop	18.18	4.91	59.31	-28.93
Others to crop	5.15	11.46	36.60	-20.38

^a Percent changes are calculated as the simulated changes in NPP, ET, and WUE due to each land conversion type and land management practices relative to background simulation experiments in MA.

^b The area ratio of a certain land conversion type to the total area where land conversion occurred in MA during 1948–2000.

stimulated most in the fertilized/irrigated cropland during early land conversion stage, while the fertilized and non-irrigated cropland obtained similar WUE capability in the late conversion stage (Figure 12). Land conversion alone decreased WUE by 10% and 11% for irrigated and non-irrigated croplands, respectively, while inclusion of nitrogen fertilizer enhanced the WUE of irrigated and non-irrigated croplands by 4% and 3%, respectively.

Combined impacts of climate, LUCC and land management on WUE

It appeared that climate change decreased NPP, ET, and WUE of terrestrial ecosystems in MA during 1948–2000, while land use and management practices alleviated these reductions (Figure 8). The largest reduction in WUE, 5.43%, occurred in the 1970s (Figure 7), when less precipitation amount significantly decreased NPP and the nitrogen fertilization effect was barely enough to reverse the LUCC-induced decline in WUE. Over the whole study period, the combined effects of climate, land conversion, and land management practices decreased WUE by 3.08%, with decreases of 0.13 and 4.63% in the 1950s and 1980s, respectively (Table II). Given the WUE change derived from these three individual factors, changes in climate, land use patterns, and management practices, the interaction among them suppressed WUE and counteracted around 20% of WUE increment due to land use and management practices.

When we went into details on land-converted areas, our simulations found that land conversion from natural vegetation to cropland generally decreased WUE by decreasing NPP and increasing ET (Figure 13). However, human perturbation complicated this pattern. It appeared that management practices were likely responsible for the unexpected changes of carbon and water interaction during land conversion. For example, only 26% of cropland was irrigated before its converting to other natural vegetation types (i.e. wetland, desert, and tundra),

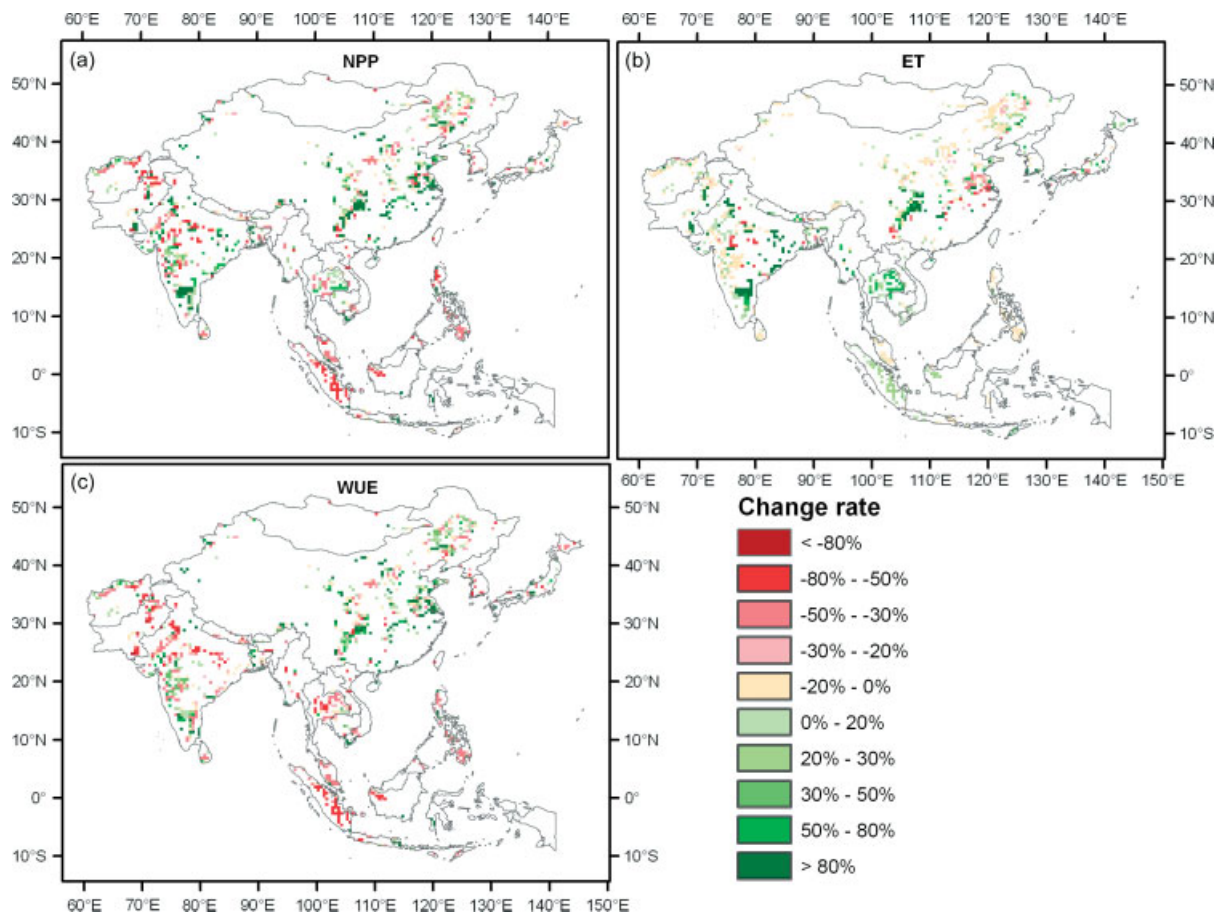


Figure 11. Changes in annual NPP (a), ET (b), and WUE (c) due to LUCC and land management practices across monsoon Asia during 1948–2000.

while 63% of land conversion from ‘other’ vegetation types to cropland was managed with irrigation. This might be part of the reason why NPP in land conversion from cropland to others, and vice versa were both subject to increase (Table III). Same patterns were found in land conversion between cropland and shrubland (Table III). Without nitrogen fertilizer application, NPP will be decreased when shrubland converting to cropland but N addition could have reversed this pattern (Figure 13(b)). Another reason is that the land conversion took place in difference regions and the differences in age as conversion would also contribute to the direction of NPP change. Therefore, it is hard to say which land cover type has higher productivity. Generally speaking, model simulations indicated that large areas of cropland establishment would lower WUE of terrestrial ecosystems of MA, but nitrogen fertilizer application might to some extent alleviate this reduction.

Climate variation showed a neutral effect or further relieved the shrink in WUE during the period when land conversion occurred from natural vegetation to cropland (Figure 13(d)). However, grassland converted to cropland is an exception where land conversion decreased ET and climate variation reduced WUE because these areas have experienced significant precipitation decrease and temperature rise in the same period when land conversion took place (Figure 13(a)). Meanwhile, our study found that only 3.7% of the cropland converted from grassland

was irrigated over the past 53 years (Figure 13(a)), which could be partly responsible for ET decrease within this type of land conversion.

On the contrary, conversion from cropland to natural vegetations increased NPP, decreased ET, and thus enhanced WUE across the study period, and climate variation has neutral or small suppressive effect on WUE increase as the newly developed shrubland, grassland and forest have experienced apparent drought conditions when land conversion occurred. Among them, conversion of cropland to grassland was another exception where ET was slightly raised by LUCC and nitrogen fertilization decreased NPP and ET (Figure 13(b)). It might be related to the fact that only 9% of those converted cropland had been irrigated before and exclusion of harvest could favour grass growth and enhance ET level. However, application of nitrogen fertilizer increased NPP of cropland before conversion, therefore, increases in NPP, ET, and consequently in WUE due to land conversion was eliminated when simultaneously considering the management effects.

DISCUSSION

Impacts of climate change

Climate exerted complex influences on carbon uptake and water use through various factors, such as

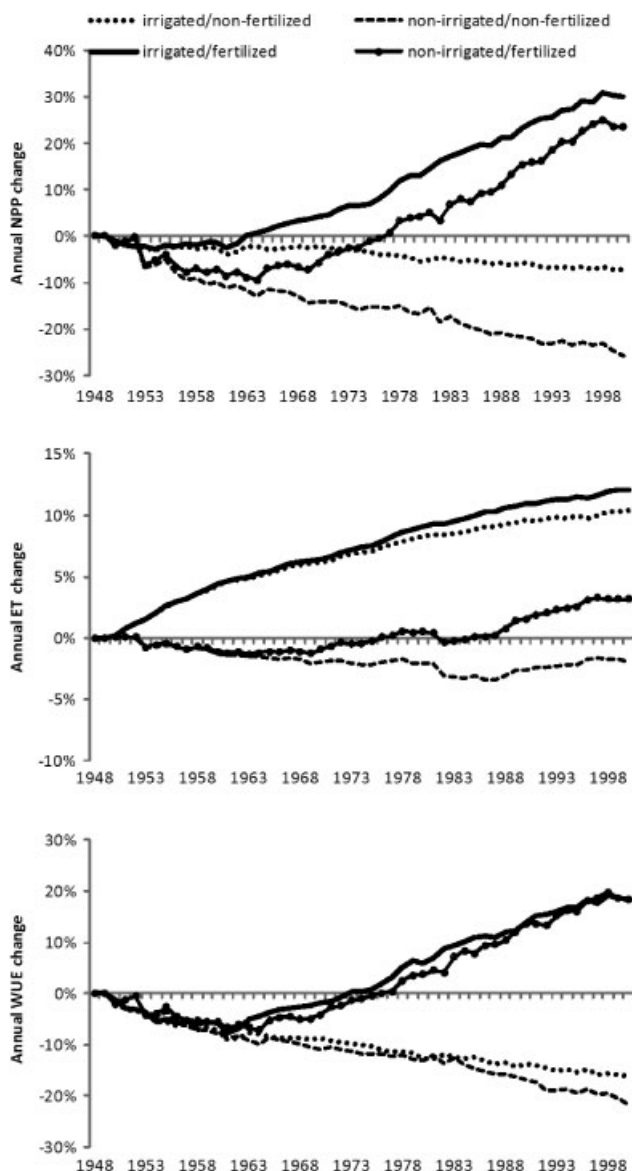


Figure 12. Changes in annual NPP, ET, and WUE induced by LUC and N fertilizer application in irrigated and non-irrigated croplands in monsoon Asia during 1948–2000.

temperature, cloudiness, water, and nutrient availability. The sensitivities of NPP to climatic changes varied among different ecosystems due to the spatial gradient of controlling factors and the ecosystems' dependence on each factor (Field *et al.*, 1992; Melillo *et al.*, 1993). Our study indicated that MA displayed a significant decrease in precipitation over the period 1948–2000, especially for the northern, northwestern, northeastern China, entire Mongolia, and large areas of India, most of which usually received less rainfall than other places (Figure 2). Similar patterns have been found by other studies (Dai *et al.*, 2004; Zou *et al.*, 2005; Xiao *et al.*, 2009). In these drying areas, our model simulations suggested a significant decline in NPP, ET, and thus WUE (Figure 10). However, NPP derived from satellite observations did not show a significant change in this area from 1982 to 1999 (Nemani *et al.*, 2003). This discrepancy is probably because other factors such as CO₂

enrichment and N deposition counteracted the NPP reduction induced by climate change. We also found that ET has significantly decreased in central MA due to precipitation decline. A recent study (Jung *et al.*, 2010) generated global ET estimate using eddy covariance data and satellite observations and did not find significant changing trend of ET in central MA since 1998, but their correlation analysis indicated ET in this area is mainly limited by moisture supply, i.e. precipitation (Figure S2 in Jung *et al.*, 2010). Overall, this reduction in NPP and ET might be related to less rainfall and more frequent drought events in MA (Xiao *et al.*, 2009), where water availability was confirmed to be the dominant environmental control to NPP (Churkina and Running, 1998). Our study found that the decrease rate of NPP was faster than that of ET, thus causing a decrease in WUE. This suggested that decrease in precipitation has a greater impact on NPP than ET. Tian *et al.* (2010a) has also found this phenomenon in the Southern United States.

In this study, we examined the relationships between changes in carbon and water fluxes and variations of temperature and precipitation. Precipitation change was found to be the dominant climatic factor, explaining 64.3%, 53.5%, and 57.5% ($p < 0.001$) of the inter-annual variations for NPP, ET, and WUE, respectively (Figure 9). Annual average temperature did not show significant correlation with the changes of these three variables, implying that changes in temperature were not the primary determinant factor for controlling inter-annual variations of NPP, ET, and WUE over MA region. Our findings also suggested that the terrestrial ecosystem in MA would be more productive and more efficient in water use in wetter years than in normal years, while WUE is less sensitive to temperature change over the past half century. This pattern was consistent with the contribution of anomalous annual precipitation and temperature to global terrestrial NPP as indicated by Mohamed *et al.* (2004). Continuous observations from three forest sites of ChinaFlux confirmed that annual average temperature and precipitation were the dominant controls to WUE in the eastern China, which can explain more than 85% of spatial variability of WUE (Yu *et al.*, 2008). Furthermore, they indicated that ecosystem WUE decreased from north to south with increasing air temperature and precipitation, and our simulations found that WUE decreased in the northern China due to expanding drought and slightly increased in the southern China due to cooling and wetting climate conditions (Figure 10).

Although DLEM used daily climate data sets and plant phenological information, we focused on the inter-annual variations of climate-induced changes in NPP, ET, and WUE in this study instead of exploring the daily or monthly patterns. We agreed with Law *et al.* (2002) that the dynamic responses related to the phenological influences at a seasonal/monthly scale could be overlooked by the analysis using annual climate information. Further studies should explore the climatic control to the carbon/water fluxes and WUE in shorter time

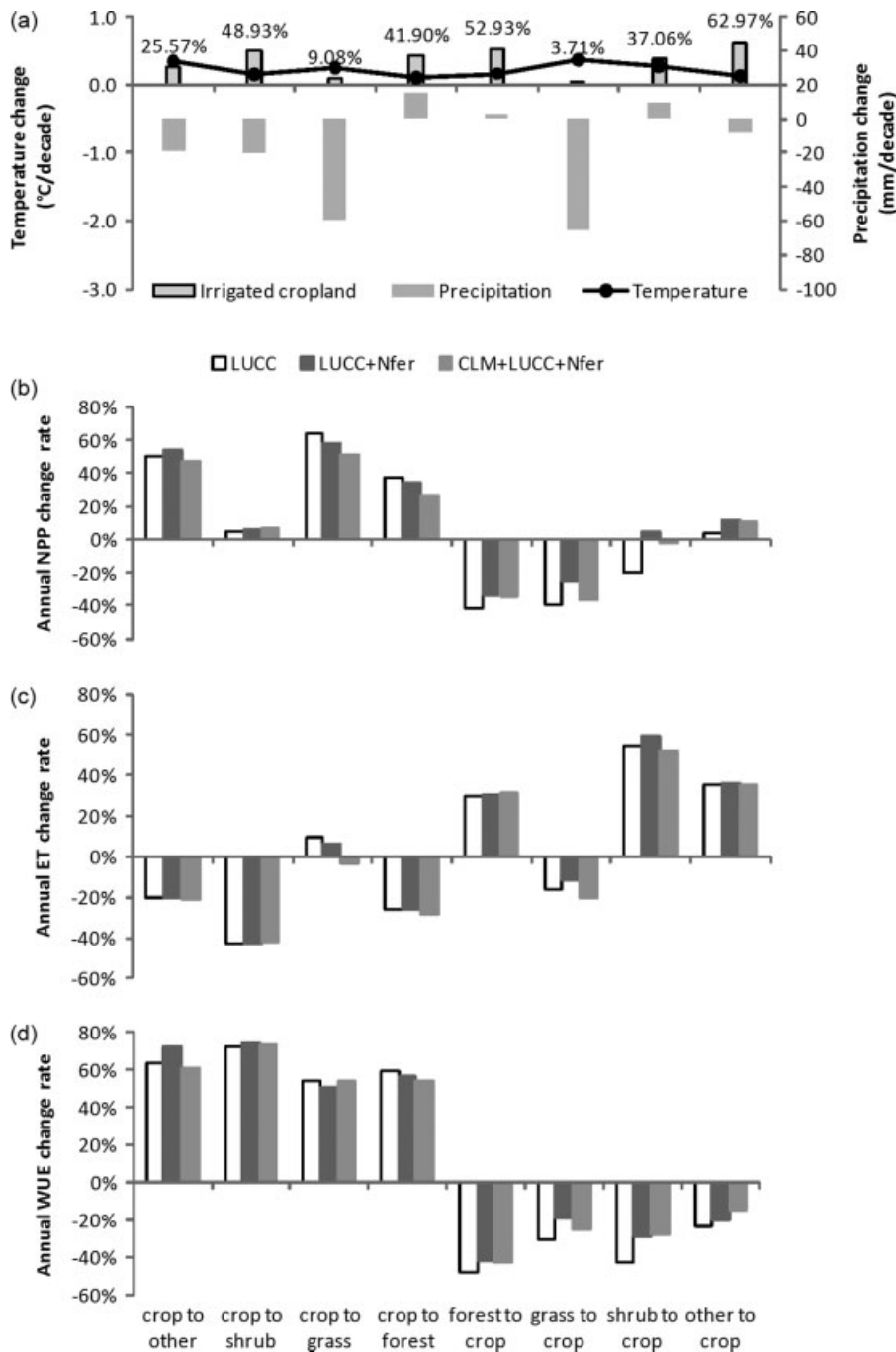


Figure 13. Interactive effects of changing climate and land use on net primary production (NPP), evapotranspiration (ET) and water use efficiency (WUE) in monsoon Asia. Changing trend of temperature and precipitation during the period when land conversion occurred and the percentage of irrigated cropland area (a), and changes in annual NPP (b), ET (c) and WUE (d) induced by climate (CLM), land conversion (LUCC) and N fertilizer application (Nfer) in each land conversion type.

steps by ecosystem type. This type of analysis is most important in the arid and semi-arid areas (Emmerich, 2007).

Impacts of LUCC and land management

WUE could be affected not only by climatic change but also by a variety of human-derived changes (Tian *et al.*, 2010a), such as land use history (Sakai *et al.*, 2004), anthropogenic disturbances including fire and harvesting (Mkhabela *et al.*, 2009). Without considering other factors, impacts of LUCC on WUE are generally determined

by the proportional distribution of different vegetation types and their sensitivities to local changes in environmental factors. We found that croplands had the lowest WUE, which was consistent with field measurements (Law *et al.*, 2002) and modelling results (Tian *et al.*, 2010a), and crop was the second most sensitive land cover type in response to climate change in MA during the study period. However, our simulations indicated that WUE of cropland gradually increased as influenced by combined factors including climate change, LUCC, and land management, with the changes ranging from

–5.24% in the 1950s to 5.06% in the 1990s. Nitrogen fertilizer application enhanced WUE for both irrigated and non-irrigated croplands through stimulating crop growth (Figure 12). Even so, expanding cropland could still lower the average WUE for the entire MA.

Bert *et al.* (1997) investigated the variations of WUE during the 20th century based on the analysis of ¹³C for tree rings of a forest ecosystem. They found that WUE increased by 30% between the 1930s and the 1980s primarily because of long-term environmental changes. Saurer *et al.* (2004) and Duquesnay *et al.* (1998) obtained similar results for forests. These studies suggested that environmental factors (such as elevated CO₂ concentration, nitrogen deposition, land management, and climate change) might also contribute to this increase in WUE. Our study indicated that changes in climate, land use and cover patterns together altered WUE in forest of MA by –12 to 8% during 1948–2000. Future work should involve more driving factors to attribute the WUE variation in this region.

Cropland management impacts on carbon and water dynamics have been intensively studied in the past decades (Li *et al.*, 2004, 2005, 2006; Lu *et al.*, 2009). One of the notable findings in this study is that ET was lower in forests than in managed cropland (Table III, Figure 13(c)), around 50% of which was irrigated before its conversion to or from forest in MA region. This might be related to huge water demands from multiple cropping systems and our model assumption of non-deficient water supply in irrigated cropland. A 5-year experiment conducted in cropland of the North China Plain (Liu *et al.*, 2002) supported this point, showing that double-cropped winter wheat and summer maize consumed 800–900 mm soil water per year with supplemental irrigation, surpassing annual precipitation by about 370 mm, or even 400 mm in dry year. However, forest that grew in the same area could not have additional water to support as much ET as managed cropland has. Besides, we found that WUE greatly increased with increasing nitrogen fertilization rate in the cropland. Combined with land conversion, the largest mean amount of nitrogen use in 2000, 78 kg N ha⁻¹ year⁻¹ enhanced WUE of croplands by nearly 20%. This implied that increasing nitrogen availability could increase efficiency of water use in both irrigated and non-irrigated cropland. A study conducted by Huxman *et al.* (2004) pointed out that that rain use efficiency (RUE, the ratio of above-ground net primary production to precipitation) decreased as mean annual precipitation increased because limitation of resources other than water, such as nitrogen, would dominate when water limitation had been relieved. They also suggested that life history and biogeochemical mechanisms interact to influence the sensitivity of NPP to precipitation, and that biomes are prone to converge at a common maximum RUE when water is the most limiting factor. However, the maximum WUE was not found in our study. It might be related to the fact that our model did not consider resources competition and vegetation dynamics in this study, therefore, the missing

of plant species with high competitive capacity and WUE could overestimate the WUE decrease in response to a drying climate.

Uncertainty

Large discrepancy was found in the existing data sets, especially LUC data, used for driving ecosystem models (Jain *et al.*, 2005; Liu and Tian, 2010). For example, Flint (1994) argued that cropland expansion only accounted for 3/4 of deforestation and the rest of declined forest area was replaced by shrubland and grassland in South and Southeast Asia from 1880 to 1980. However, our LUC data, developed from HYDE v3.0 global cropland distribution data (Goldewijk, 2001), showed that large areas of forest, shrubland and grassland was replaced by agricultural land and we found shrubland and grassland areas decreased during 1948–2000. Several points might be responsible for this data set inconsistency: (1) different geographical boundary for South and Southeast Asia (13 countries for Flint, (1994) and 15 countries in this study); (2) different study period; and (3) different definition for shrubland and grassland, which includes non-forested wetlands in Flint, (1994). It is notable that we did not include the land conversion among natural vegetation types due to a lack of long-term records on deforestation, afforestation/reforestation, and grassland degradation in the MA region. If part of forest was converted to shrubland and grassland as suggested by Flint (1994), rather than to managed cropland, our model simulations probably overestimated the WUE increase induced by LUC and land management practices. Therefore, a well-refined, consistent LUC data set is in an urgent need for accurately quantifying the WUE change in response to human activities.

Currently, about 50% of cropland in MA is rainfed, and half of the rainfed cropland is located in the arid or semi-arid areas. We found that WUE was higher in the irrigated cropland than that in the non-irrigated cropland (Figure 12), which was consistent with many previous studies (Hsiao, 1973; Howell, 2001). However, in this study, the irrigated water was assumed to increase soil moisture to the level of field capacity for each irrigation event. This means that no runoff loss occurred during irrigation practices, resulting in a higher WUE. This model assumption also reduced drought damage and overestimated WUE in cropland of arid region that could experience periodic drought stress even under irrigation. Further study is needed to improve model simulation for irrigation impacts.

Model structure, assumptions, and parameter estimates composed additional uncertainty sources of model outputs. Further efforts need to emphasize model–model intercomparison to identify and quantify the likely uncertainties caused by different modelling schemes. Besides, we call for more field experiments involving both climate conditions and anthropogenic disturbances to better understand the underlying mechanisms and calibrate and validate the model behaviours.

CONCLUSION

We investigated the effects of climate change, LUCC, and land management practices on the interactions of terrestrial carbon and water fluxes in terms of WUE in MA during 1948–2000. Simulated results indicate that climate variability/change during 1948–2000 led to WUE decrease at the continental level, but varied greatly across the region. WUE in northern China and entire Mongolia appeared to have larger response to climate change, with a decrease of more than 50%, while WUE change was much less in the southern MA including part of southern China and Southeast Asia. By contrast, WUE in the southern and western China, and most areas of India increased by more than 30% as influenced by climate change. In the areas where LUCC occurred, cropland establishment substantially decreased WUE by 15–42%, while it was increased by 54–73% for land conversion from cropland to natural vegetation. Throughout the late half of the 20th century, cropland expansion in the arid and semi-arid areas might be responsible for the significant decrease of WUE in MA. Our study also suggested that land management practices, including fertilization and irrigation, could alleviate or even overturn the WUE reduction induced by climate change and land conversions.

This study indicated that climate change played a critical role in determining WUE change over the entire MA region during the late half of the 20th century. Although impacts of LUCC on WUE appeared relatively small compared to those of climate change on the continental scale, our study showed that LUCC had much larger influences than climate in the areas where LUCC occurred. This implied that WUE would be largely determined by human activities if land conversion continued to expand in the future. In addition, we found that appropriate irrigation and fertilizer application could increase WUE and counteract the decreasing trend of WUE induced by climate change and LUCC. However, the extra fertilized nitrogen or irrigated water that cannot be taken up by crop will pollute the freshwater systems and lead to soil salination. Appropriate irrigation (timing, quantity, and irrigation systems) and fertilization (amount and timing) are necessary to maintain high crop productivity, reduce fresh water use, maximize WUE and minimize soil and water pollution.

Future studies should explore the interactive effects of multiple environmental stresses on carbon and water linkage through integrated modelling and manipulated experiments. Appropriate management strategies should be identified and extensively evaluated to figure out an effective way for using freshwater, especially in human-dominated, or vulnerable ecosystems in face of frequent drought events.

ACKNOWLEDGEMENTS

This study has been supported by NASA Land Cover/Land Use Change Program (NNX08AL73G-S01), NASA

InterDisciplinary Science (IDS) Program (NNG04GM 39C) and the National Basic Research Program of China (No.2010CB950900). We thank Dr James Vose, Kamaljit Banger, and two anonymous reviewers for their constructive comments.

REFERENCES

- Bert GD, Leavitt SW, Dupouey JL. 1997. Variations of wood ¹³C and water-use efficiency of *Abies alba* (Mill.) during the last century. *Ecology* **78**: 1588–1596.
- Bliss NB, Olsen LM. 1996. Development of a 30-arc-second digital elevation model of South America. In Pecora Thirteen, Human Interactions with the Environment—Perspectives from Space, Sioux Falls, South Dakota.
- Bonan GB. 1996. A land surface model (LSM version 1.0) for ecological, hydrological, and atmospheric studies: technical description and user's guide, NCAR/TN-417+STR, NCAR Technical Note, Boulder, Colorado.
- Chen G, Tian H, Liu M, Ren W, Zhang C, Pan S. 2006. Climate impacts on China's terrestrial carbon cycle: an assessment with the dynamic land ecosystem model. In *Environmental Modeling and Simulation*, Tian HQ (ed). ACTA Press: Calgary; 56–70.
- Churkina G, Running S. 1998. Contrasting climatic controls on the estimated productivity of global terrestrial biomes. *Ecosystems* **1**: 206–215.
- Collatz GJ, Ball JT, Grivet C, Berry JA. 1991. Physiological and environmental regulation of stomatal conductance, photosynthesis and transpiration: A model that includes a laminar boundary layer. *Agricultural and Forest Meteorology* **54**: 107–136.
- Dai A, Kevin ET, Qian T. 2004. A global dataset of Palmer Drought Severity Index for 1870–2002: relationship with soil moisture and effects of surface warming. *Journal of Hydrometeorology* **5**: 1117–1130.
- Davi H, Dufrene E, Francois C, Le Maire G, Loustau D, Bosc A, Rambal S, Granier A, Moors E. 2006. Sensitivity of water and carbon fluxes to climate changes from 1960 to 2100 in European forest ecosystems. *Agriculture and Forest Meteorology* **141**: 35–56.
- Duquesnay A, Breda N, Stievenard M, Dupouey JL. 1998. Changes of tree-ring δ^{13} C and water-use efficiency of beech (*Fagus sylvatica* L.) in north-eastern France during the past century. *Plant, Cell and Environment* **21**: 565–572.
- Emmerich WE. 2007. Ecosystem water use efficiency in a semiarid shrubland and grassland community. *Rangeland Ecology & Management* **60**: 464–470.
- Farquhar GD, von Caemmerer S, Berry JA. 1980. A biochemical model of photosynthetic CO₂ assimilation in leaves of C₃ species. *Planta* **149**: 78–90.
- Field C, Chapin FS III, Matson PA, Mooney HA. 1992. Responses of terrestrial ecosystems to the changing atmosphere: a resource-based approach. *Annual Review of Ecology and Systematics* **23**: 201–235.
- Flint EP. 1994. Changes in land use in South and Southeast Asia from 1880–1980: a data base prepared as part of coordinated research program on carbon fluxes in the tropics. *Chemosphere* **29**: 1015–1062.
- Gerten D, Luo Y, Le Maire G, Parton W, Keough C, Weng E, Beier C, Cias P, Cramer W, Dukes J, Hanson P, Knapp A, Linder S, Nepstad D, Rustad L, Sowerby A. 2008. Modelled effects of precipitation on ecosystem carbon and water dynamics in different climatic zones. *Global Change Biology* **14**: 2365–2379.
- Goldewijk K. 2001. Estimating global land use change over the past 300 years: the HYDE database. *Global Biogeochemical Cycles* **15**: 417–434.
- Haefner JW. 2005. Modeling biological systems: principles and applications. New York: Springer Science + Business Media.
- Houghton RA, Hackler JL. 2003. Sources and sinks of carbon from land-use change in China. *Global Biogeochemical Cycles* **17**: 1034.
- Houghton RA, Hobbie JE, Melillo JM, Moore B, Peterson BJ, Shaver GR, Woodwell *et al.* 1983. Changes in the carbon content of terrestrial biota and soils between 1860 and 1980: a net release of CO₂ to the atmosphere. *Ecological Monographs* **53**(3): 235–262.
- Howell TA. 2001. Enhancing water use efficiency in irrigated agriculture. *Agronomy Journal* **93**: 281–289.
- Hsiao TC. 1973. Plant responses to water stress. *Annual Review of Plant Physiology* **24**: 519–570.
- Huxman TE, Smith MD, Fay PA, Knapp AK, Shaw MR, Loik ME, Smith SD, Tissue DT, Zak JC, Weltzin JF, Pockman WT, Sala OE, Haddad

- BM, Harte J, Koch GW, Schwinning S, Small EG, Williams DG. 2004. Convergence across biomes to a common rain-use efficiency. *Nature* **429**: 651–654.
- Jain AK, Yang X. 2005. Modeling the effects of two different land cover change data sets on the carbon stocks of plants and soils in concert with CO₂ and climate change. *Global Biogeochemical Cycles* **19**: GB2015. DOI: 10.1029/2004GB002349.
- Jarosz N, Béziat P, Bonnefond J-M, Brunet Y, Calvet J-C, Ceschia E, Elbers JA, Hutjes RWA, Traullé O. 2009. Effect of land use on carbon dioxide, water vapour and energy exchange over terrestrial ecosystems in Southwestern France during the CERES campaign. *Biogeosciences Discuss* **6**: 2755–2784.
- Jung M, Reichstein M, Ciais P, Seneviratne S, Sheffield J, Goulden M, Bonan GB, Cescatti A, Chen J, de Jeu R, Dolman AJ, Eugster W, Gerten D, Gianelle D, Gobron N, Heinke J, Kimball JS, Law BE, Montagnani L, Mu Q, Mueller B, Oleson KW, Papale D, Richardson AD, Rouspard O, Running SW, Tomelleri E, Viovy N, Weber U, Williams C, Wood E, Zaehle S, Zhang K. 2010. Recent decline in the global land evapotranspiration trend due to limited moisture supply. *Nature* **467**: 951–954.
- Lal M, Harasawa H, Murdiyarsa D, et al. 2001. Asia. In *Climate Change 2001: Impacts, Adaptation, and Vulnerability. Third Assessment Report of the Intergovernmental Panel on Climate Change*. McCarthy JJ, Canziani OF, Leary NA, Dokken DJ, White KS (eds). Cambridge University Press: Cambridge, UK; 533–590.
- Law B, Falge E, Gu L, Baldocchi D, Bakwin P, Berbigier P, Davis K, Dolman A, Falk M, Fuentes J, Goldstein A, Granier A, Grelle A, Hollinger D, Janssens I, Jarvis P, Jensen N, Katul G, Mahli Y, Metteucci G, Meyers T, Monson R, Munger W, Oechel W, Olson R, Pilegaard K, Paw K, Thorgeirsson H, Valentini R, Verma S, Vesala T, Wilson K, Wofsy S. 2002. Environmental controls over carbon dioxide and water vapor exchange of terrestrial vegetation. *Agriculture and Forest Meteorology* **113**: 97–120.
- Leff B, Ramankutty N, Foley JA. 2004. Geographic distribution of major crops across the world. *Global Biogeochemical Cycles* **18**: GB1009. DOI: 10.1029/2003GB002108.
- Lehner B, Döll P. 2004. Development and validation of a global database of lakes, reservoirs and wetlands. *Journal of Hydrology* **296**: 1–22.
- Li C, Cui J, Sun G, Trettin C. 2004. Modeling impacts of management on carbon sequestration and trace gas emissions in forested wetland ecosystems. *Environmental Management* **33**: 176–186. DOI: 10.1007/s00267-003-9128-z.
- Li C, Frolking S, Xiao X, Moore B III, Boles S, Qiu J, Huang Y, Salas W, Sass R. 2005. Modeling impacts of farming management alternatives on CO₂, CH₄, and N₂O emissions: a case study for water management of rice agriculture of China. *Global Biogeochemical Cycles* **19**: GB3010. DOI: 10.1029/2004GB002341.
- Li C, Salas W, DeAngelo B, Rose S. 2006. Assessing alternatives for mitigating net greenhouse gas emissions and increasing yields from rice production in China over the next 20 years. *Journal of Environmental Quality* **35**: 1554–1565. DOI: 10.2134/jeq2005.0208.
- Li J, Erickson J, Peresta G, Drake B. 2010. Evapotranspiration and water use efficiency in a Chesapeake Bay wetland under carbon dioxide enrichment. *Global Change Biology* **16**: 234–245.
- Liang N, Maruyama K. 1995. Interactive effects of CO₂ enrichment and drought stress on gas exchange and water-use efficiency in *Alnus Firma*. *Environmental and Experimental Botany* **35**: 353–361.
- Lim CFA, Suzuki M, Ohte N, Hotta N, Kume T. 2009. Evapotranspiration patterns for tropical rainforests in Southeast Asia: a model performance examination of the Biome-BGC model. *Bulletin of the Tokyo University Forests* **120**: 29–44.
- Liu JG, Diamond J. 2005. China's environment in a globalizing world. *Nature* **435**: 1179–1186.
- Liu M, Tian HQ. 2010. China's land-cover and land-use change from 1700 to 2005: estimations from high-resolution satellite data and historical archives. *Global Biogeochemical Cycles* **24**: GB3003. DOI: 10.1029/2009GB003687.
- Liu CM, Zhang XY, Zhang YQ. 2002. Determination of daily evaporation and evapotranspiration of winter wheat and maize by large-scale weighing lysimeter and micro-lysimeter. *Agriculture and Forest Meteorology* **111**: 109–120.
- Liu M, Tian HQ, Chen GS, Ren W, Zhang C, Liu J. 2008. Effects of land use/cover change on evapotranspiration and water yield in China during the 20th century. *Journal of the American Water Resources Association (JAWRA)* **44**(5): 1193–1207.
- Lu F, Wang X, Han B, Quyang Z, Duan X, Zheng H, Miao H. 2009. Soil carbon sequestrations by nitrogen fertilizer application, straw return and no-tillage in China's cropland. *Global Change Biology* **15**: 281–305.
- Luo Y, Gerten D, Le Maire G, Parton W, Weng E, Zhou X, Keough C, Beier C, Cias P, Cramer W, Dukes J, Emmett B, Hanson P, Knapp A, Linder S, Nepstad D, Rustad L. 2008. Modeled interactive effects of precipitation, temperature, and CO₂ on ecosystem carbon and water dynamics in different climatic zones. *Global Change Biology* **14**: 1986–1999.
- McGuire AD, Sitch S, Clein JS, Dargaville R, Esser G, Foley J, Heimann M, Joos F, Kaplan J, Kicklighter DW, Meier RA, Melillo JM, Moore B III, Prentice IC, Ramankutty N, Reichenau T, Schloss A, Tian H, Williams LJ, Wittenberg U. 2001. Carbon balance of the terrestrial biosphere in the twentieth century: analyses of CO₂, climate and land-use effects with four process-based ecosystem models. *Global Biogeochemical Cycles* **15**: 183–206.
- Meehl GA, Stocker TF, Collins WD, Friedlingstein P, Gaye AT, Gregory JM, Kitoh A, Knutti R, Murphy JM, Noda A, Raper SCB, Watterston IG, Weaver AJ, Zhao Z-C. 2007. Global climate projections. In *Climate Change 2007: The Physical Science Basis. Contribution of Working Group I to the Fourth Assessment Report of the Intergovernmental Panel on Climate Change*. Solomon S, Qin D, Manning M, Chen Z, Marquis M, Averyt KB, Tignor M, Miller HL (eds). Cambridge University Press: Cambridge, United Kingdom and New York, NY, USA; 748–845.
- Melillo JM, McGuire AD, Kicklighter DW, Moore B III, Vörösmarty CJ, Schloss AL. 1993. Global climate change and terrestrial net primary production. *Nature* **363**: 234–240.
- Mkhabela MS, Amiro B, Barr A, Black T, Hawthorne I, Kidston J, McCaughey J, Orchansky A, Nescic Z, Sass A, Shashkov A, Zha T. 2009. Comparison of carbon dynamics and water use efficiency following fire and harvesting in Canadian boreal forests. *Agricultural and Forest Meteorology* **149**: 783–794.
- Mohamed M, Babiker IS, Chen ZM, Ikeda K, Ohta K, Kato K. 2004. The role of climate variability in the inter-annual variation of terrestrial net primary production (NPP). *Science of the Total Environment* **332**: 123–137.
- Mu Q, Zhao M, Running SW, Liu M, Tian H. 2008. Contribution of increasing CO₂ and climate change to the carbon cycle in China's ecosystems. *Journal of Geophysical Research* **113**: G01018. DOI: 10.1029/2006JG000316.
- Nemani RR, Keeling CD, Hashimoto H, Jolly WM, Piper SC, Tucker CJ, Myeni RB, Running SW. 2003. Climate-driven increases in global terrestrial net primary production from 1982 to 1999. *Science* **300**: 1560–1563.
- Oikawa T, Ito A. 2001. Modeling carbon dynamics of terrestrial ecosystems in Monsoon Asia. In *Present and Future Modeling Global Environmental Change: Toward Integrated Modeling*. Matsuno T, Kida H (eds). Terrapub: Tokyo; 207–219.
- Oleson K, Dai Y, Bonan G, Bosilovich M, Dickinson R, Dirmeyer P, Hoffman F, Houser P, Levis S, Niu GY, Thornton P, Verstein M, Yang ZL, Zeng XB. 2004. Technical description of the community land model (CLM). Technical Note NCAR/TN-461+STR, National Center for Atmospheric Research.
- Olson RJ, Scurlock JMO, Prince SD, Zheng DL, Johnson KR, (eds) 2001. *NPP multi-biome: global primary production data initiative products*. Available on-line (<http://www.daac.ornl.gov/>) from the Oak Ridge National Laboratory Distributed Active Archive Center, Oak Ridge, Tennessee, USA [last accessed 3/13/2011].
- Ramankutty N, Foley J. 1999. Estimating historical changes in global land cover: Croplands from 1700 to 1992. *Global Biogeochemical Cycles* **13**: 997–1027.
- Ren W, Tian H, Liu M, Zhang C, Chen G, Pan S, Felzer B, Xu X. 2007. Effects of tropospheric ozone pollution on net primary productivity and carbon storage in terrestrial ecosystems of China. *Journal of Geophysical Research* **112**: D22S09. DOI: 10.1029/2007JD008521.
- Ren W, Tian H, Xu X, Liu M, Lu C, Chen G, Mellio J, Reilly J, Liu J. 2011. Spatial and temporal patterns of CO₂ and CH₄ fluxes in China's croplands in response to multifactor environmental changes. *Tellus B* DOI: 10.1111/j.1600-0889.2010.00522.x.
- Sakai R, Fitzjarrald D, Moraes O, Staebler R, Acevedo O, Czikowsky M, Silva R, Brait E, Miranda V. 2004. Land-use change effects on local energy, water, and carbon balance in an Amazonian agricultural field. *Global Change Biology* **10**: 895–907.
- Saurer M, Siegwolf RTW, Schweingruber FH. 2004. Carbon isotope discrimination indicates improving water-use efficiency of trees in northern Eurasia over the last 100 years. *Global Change Biology* **10**: 2109–2120.
- Schimmel DS, Braswell BH, Parton WJ. 1997. Equilibration of the terrestrial water, nitrogen, and carbon cycles. *Proceedings of the National Academy of Sciences* **94**: 8280–8283.

- Schwalm CR, Williams CA, Schaefer K, Anderson R, Arain MA, Baker I, Black TA, Chen G, Ciais P, Davis KJ. Other NACP participants. 2010. A model-data intercomparison of CO₂ exchange across North America: Results from the North American Carbon Program Site Synthesis. *Journal of Geophysical Research* **115**: G00H05. DOI: 10.1029/2009JG001229.
- Sellers PJ, Berry JA, Collatz GJ, Field CB, Hall FG. 1992. Canopy reflectance, photosynthesis and transpiration, III. A reanalysis using improved leaf models and a new canopy integration scheme. *Remote Sensing of Environment* **42**: 1–20.
- Siebert S, Döl P, Feick S, Frenken K, Hoogeveen J. 2007. Global map of irrigation areas version 4.0.1. University of Frankfurt (Main), Germany, and FAO, Rome, Italy. <http://www.fao.org/nr/water/aquastat/irrigationmap/index.stm> [last accessed 3/13/2011].
- Song ZW, Zhang HL, Snyder RL, Anderson FE, Chen F. 2010. Distribution and trends in reference evapotranspiration in the North China Plain. *Journal of Irrigation and Drainage Engineering* **136**: 240–247.
- Still CJ, Berry JA, Collatz GJ, DeFries RS. 2003. Global distribution of C3 and C4 vegetation: Carbon cycle implications. *Global Biogeochemical Cycles* **17**: 1006. DOI: 10.1029/2001GB001807.
- Theil H. 1961. *Economic forecasts and policy*. (2nd ed.) Amsterdam, NE: North-Holland.
- Tian H, Chen G, Liu M, Zhang C, Sun G, Lu C, Xu X, Ren W, Pan S, Chappelka A. 2010a. Model estimates of ecosystem net primary productivity, evapotranspiration, and water use efficiency in the southern United States during 1895–2007. *Forest Ecology and Management* **259**: 1311–1327.
- Tian HQ, Xu XF, Liu ML, Ren W, Zhang C, Chen G, Lu C. 2010b. Spatial and temporal patterns of CH₄ and N₂O fluxes in terrestrial ecosystems of North America during 1979–2008: application of a global biogeochemistry model. *Biogeosciences* **7**: 2673–2694.
- Tian H, Liu J, Melillo JM, Liu M, Kicklighter D, Yan X, Pan S. 2008. The terrestrial carbon budget in East Asia: human and natural impacts. In *Changes in the Human-Monsoon System of East Asia in the Context of Global Change*. Fu C, Freney J, Steward J (eds). World Scientific Publishing Co. Pte.Ltd.: Singapore, Hackensack, London; 163–176.
- Tian H, Melillo J, Kicklighter D, Pan S, Liu J, McGuire AD, Moore B III. 2003. Regional carbon dynamics in monsoon Asia and its implications to the global carbon cycle. *Global and Planetary Change* **37**: 201–217.
- Tian HQ, Melillo J, Lu CQ, Kicklighter D, Liu ML, Ren W, Xu XF, Chen GS, Zhang C, Pan SF, Liu JY, Running S. 2011a. China's terrestrial carbon balance: contributions from multiple global change factors. *Global Biogeochemical Cycles* DOI:10.1029/2010GB003838.
- Tian HQ, Xu X, Liu M, Lu C, Ren W, Chen G, Melillo J, Liu J. 2011b. Net exchanges of CO₂, CH₄, and N₂O between China's terrestrial ecosystems and the atmosphere and their contributions to global climate warming. *Journal of Geophysical Research* DOI:10.1029/2010JG001393.
- Trenberth KE, Jones PD, Ambenje P, Bojariu R, Easterling D, Klein Tank A, Parker D, Rahimzadeh F, Renwick JA, Rusticucci M, Soden B, Zhai P. 2007. Observations: surface and atmospheric climate change. In *Climate Change 2007: The Physical Science Basis. Contribution of Working Group I to the Fourth Assessment Report of the Intergovernmental Panel on Climate Change*. Solomon S, Qin D, Manning M, Chen Z, Marquis M, Averyt KB, Tignor M, Miller HL (eds). Cambridge University Press: Cambridge, United Kingdom and New York, NY, USA; 236–336.
- Wang J, Yu G, Fang Q, Jiang D, Qi H, Wang Q. 2008. Responses of water use efficiency of 9 plant species to light and CO₂ and their modeling. *Acta Ecologica Sinica* **28**: 525–533.
- Waring RH, Running SW. 1998. *Forest Ecosystems Analysis at Multiple Scales*. Academic Press: San Diego, CA; 370.
- Xiao J, Zhuang Q, Liang E, McGuire A, Moody A, Kicklighter A, Shao X, Melillo J. 2009. Twentieth-century droughts and their impacts on terrestrial carbon cycling in China. *Earth Interaction* **13**: 1–31.
- Xu X, Tian H, Zhang C, Liu M, Ren W, Chen G, Lu C, Bruhwiler L. 2010. Attribution of spatial and temporal variations in terrestrial methane flux over North America. *Biogeosciences Discuss* **7**: 5383–5428. DOI: 10.5194/bgd-7-1-2010.
- Yu GR, Song X, Wang QF, Liu YF, Guan DX, Yan JH, Sun XM, Zhang LM, Wen XF. 2008. Water-use efficiency of forest ecosystems in eastern China and its relations to climatic variables. *New Phytologist* **177**: 927–937.
- Zhang C, Tian HQ, Pan S, Liu M, Lockaby G, Schilling EB, Stanturf J. 2008a. Effects of forest regrowth and urbanization on ecosystem carbon storage in a rural–urban gradient in the Southeast US. *Ecosystems* **11**: 1211–1222.
- Zhang YQ, Yu Q, Jiang J, Tang YH. 2008b. Calibration of Terra/MODIS gross primary production over an irrigated cropland on the North China Plain and an alpine meadow on the Tibetan Plateau. *Global Change Biology* **14**: 757–767.
- Zhang F, Li C, Wang Z, Wu H. 2006. Modeling impacts of management alternatives on soil carbon storage of farmland in Northwest China. *Biogeosciences* **3**: 451–466.
- Zhang J, Hu Y, Xiao X, Chen P, Han S, Song G, Yu G. 2009. Satellite-based estimation of evapotranspiration of an old-growth temperate mixed forest. *Agricultural and Forest Meteorology* **149**: 976–984.
- Zhao M, Heinsch F, Remani R, Running S. 2005. Improvements of the MODIS terrestrial gross and net primary production global data set. *Remote Sensing of Environment* **95**: 164–176.
- Zou X, Zhai P, Zhang Q. 2005. Variations in droughts over China: 1951–2003. *Geophysical Research Letters* **32**: L04707. DOI: 10.1029/2004GL021853.